

**EFFICIENCY IMPROVEMENT OF A DYE SENSITIZED
SOLAR CELL USING GREEN SYNTHESIZED SILVER
NANOPARTICLE**

BY

JAWONDO ASHIAT SULEIMAN

(16/27/MPH002)

**A DISSERTATION SUBMITTED TO THE
DEPARTMENT OF PHYSICS AND MATERIAL SCIENCE,
COLLEGE OF PURE AND APPLIED SCIENCE
KWARA STATE UNIVERSITY, MALETE,
NIGERIA.**

**IN PARTIAL FULFILLMENT OF THE REQUIREMENTS
FOR THE AWARD OF MASTER OF SCIENCE (M.SC.)
DEGREE IN PHYSICS AND MATERIAL SCIENCE.**

AUGUST, 2018.

ProQuest Number: 10974459

All rights reserved

INFORMATION TO ALL USERS

The quality of this reproduction is dependent upon the quality of the copy submitted.

In the unlikely event that the author did not send a complete manuscript and there are missing pages, these will be noted. Also, if material had to be removed, a note will indicate the deletion.



ProQuest 10974459

Published by ProQuest LLC (2018). Copyright of the Dissertation is held by the Author.

All rights reserved.

This work is protected against unauthorized copying under Title 17, United States Code
Microform Edition © ProQuest LLC.

ProQuest LLC.
789 East Eisenhower Parkway
P.O. Box 1346
Ann Arbor, MI 48106 – 1346

CERTIFICATION

This dissertation titled “Efficiency Improvement Of A Dye Sensitized Solar Cell Using Green Synthesized Silver Nanoparticle” by Suleiman, Jawondo Ashiat has met all the requirements for the award of degree of Master of Science in Physics and Material Science of Kwara State University, Malete, and is approved for its contribution to knowledge.

PROF. A. O. AINA
MAJOR SUPERVISOR

DATE

DR. Y.K. SANUSI
CO-SUPERVISOR

DATE

PROF. A. O. AINA
HEAD OF DEPARTMENT

DATE

PROF. S. K. SUBAIR
DEAN OF POSTGRADUATE SCHOOL

DATE

DEDICATION

This project work is dedicated to Almighty God who bestowed on me, knowledge, wisdom and understanding throughout the period of the M.Sc. programme.

ACKNOWLEDGEMENT

All thanks to God, the Almighty for giving me the strength, wisdom, knowledge and understanding towards completing this project work successfully.

My profound gratitude goes to my supervisor, Dr. Y.K. Sanusi, who went through my project work and make corrections where necessary for the success of the Masters of Science in Physics and Material Science, may almighty God bless you.

I wish to express my appreciation to all the lecturers in the department, starting with the Head of the Department, Prof. A.O. Aina, Postgraduate Coordinator and other distinguished lecturers and non-academic members of staff, I say a big thank you for making my stay worthwhile. I am very grateful, may God bless you all.

In addition, my appreciation goes to the staff of Material Science Laboratory department. It would not have been so rewarding without these people: Mr. Sunday Wilson Balogun, Engr. Abdulrasheed and Mr. Shina. I must mention my deep sense of appreciation to Dr. Alabi, Mr. Ezike, and Mr. Abdul-Rahuf Feyitimi. Thank you for your support and advice during the course of this project.

To the most caring parents in the world: ALHAJI & ALHAJA SULEIMAN JAWONDO for their love, concern and contribution to the success of this programme, may almighty Allah continue to bless you abundantly. Amen!

I also wish to appreciate my siblings, Mrs. Abdulraheem, Mrs. Abdulmalik, and others, for their love and kindness during hard times. May almighty God reward you in abundance.

To all my friends, colleagues, especially the postgraduate class members and many that contributed one way or the other to the success of this work, may God bless you abundantly.

ABSTRACT

Development of highly efficient dye-sensitized solar cells (DSSCs) with good photovoltaic parameters is an active research area of current global interest. Recently, one dimensional nanomaterial, such as silver, gold and other highly conductive metals nanoparticles are used in DSSCs anode because of their ability to improve the electron transport leading to enhanced electron collection efficiency. In the present work, the effect of green synthetic silver nanoparticles using caricapapaya leaves for conversion efficiency enhancement of dye sensitized solar cells was investigated. Studies of the influence of the structural and optical properties of the silver nanoparticles were carried out using UV-Vis spectroscopy and scanning electron microscopy, respectively. Electrical characteristics with and without the presence of metallic nanostructures were analyzed using the I-V Characteristics to observe the plasmonic effects of silver nanoparticles on the performance of photoanode in the solar cells. The total photon-to-current energy conversion efficiency obtained for the fluorine doped tin oxide/Titanium dioxide (FTO/TiO₂) and fluorine doped Tin oxide/Titanium dioxide/Silver Nanoparticles (FTO/TiO₂/Ag-NPs) electrodes were 8.90% and 10.32%, respectively, taking into consideration the optimum thickness, dye-loading time and annealing temperature as specification factors. The results reveal that adding silver nanoparticles (Ag-NPs) to Titanium dioxide(TiO₂) photoanode significantly improved the performance of the DSSC. The FTO/TiO₂/Ag-NP electrode presents an enhanced photocurrent response compared to the FTO/TiO₂ electrode. The cell with FTO/TiO₂/Ag-NP electrode exhibited over 20% improvement over the photocurrent of FTO-based device lacking silver nanoparticles. The feasibility of using locally available material for synthesizing silver nanoparticles for enhancement in performance of the photoanode of DSSC was established in this work.

TABLE OF CONTENTS

| | |
|-------------------------|-----|
| Title Page..... | i |
| Certification..... | ii |
| Dedication..... | iii |
| Acknowledgement..... | iv |
| Abstract..... | v |
| Table of Contents..... | vi |
| List of Tables..... | ix |
| List of Figures..... | x |
| List of Appendices..... | xii |

CHAPTER ONE

| | |
|-------------------------------------|---|
| 1.1 Introduction..... | 1 |
| 1.2 Statement of the problem..... | 3 |
| 1.3 Justification of the study..... | 3 |
| 1.4 Aims of the study..... | 4 |
| 1.5 Objectives of the study..... | 4 |
| 1.6 Significance of the study..... | 4 |
| 1.7 Scope of study..... | 5 |

CHAPTER TWO

| | |
|---|---|
| 2.0 Literature review..... | 6 |
| 2.1 Solar Cells..... | 6 |
| 2.2 First Generation Solar Cell-Wafer Based | 6 |
| 2.2.1 Single/Mono-Crystalline Silicon Solar Cell..... | 7 |
| 2.2.2 Polycrystalline Silicon Solar Cell (Poly-Si or Mc-Si) | 7 |

| | | |
|----------------------|---|----|
| 2.3 | Second Generation Solar Cells-Thin Film Solar Cells..... | 7 |
| 2.3.1 | Amorphous Silicon Thin Film (a-Si) Solar Cell..... | 8 |
| 2.3.2 | Cadmium Telluride (CdTe) Thin Film Solar Cell..... | 8 |
| 2.3.3 | Copper Indium Gallium Di-Selenide (CIGS) Solar Cells..... | 9 |
| 2.4 | Third Generation Solar Cells..... | 10 |
| 2.4.1 | Nano Crystal Based Solar Cells..... | 10 |
| 2.4.2 | Polymer Solar Cells..... | 11 |
| 2.4.3 | Dye Sensitized Solar Cells (DSSC)..... | 12 |
| 2.4.4 | Concentrated Solar Cells..... | 13 |
| 2.5 | Perovskite Based Solar Cell..... | 14 |
| 2.6 | Characterization of Solar Cells..... | 14 |
| 2.7 | Solar Cells Efficiency..... | 17 |
| 2.7.1 | Cell Temperature..... | 17 |
| 2.7.2 | Energy Conversion Efficiency..... | 19 |
| 2.7.3 | Maximum Power Point Tracking..... | 20 |
| 2.8 | Review of Some Related Research Works..... | 22 |
| CHAPTER THREE | | |
| 3.0 | Materials and methods..... | 25 |
| 3.1 | Materials..... | 25 |
| 3.2 | Equipment..... | 25 |
| 3.3 | Synthesis of Silver Nanoparticles | 28 |
| 3.4 | Substrate Purification..... | 28 |
| 3.5 | Preparation of Silver Nanoparticles Thin Film..... | 29 |
| 3.6 | Preparation of Silver Nanoparticles and TiO ₂ Composite Thin Film..... | 29 |

| | | |
|-------------------------|---|----|
| 3.7 | Characterization of Structure and Optical Properties of Silver Nanoparticles..... | 29 |
| 3.8 | Preparation of Conductive Glasses (FTO)..... | 30 |
| 3.9 | Preparation of Working Electrode (Anode) | 30 |
| 3.9.1 | Determination of Thickness of the Film..... | 31 |
| 3.9.2 | Dye Loading Time..... | 32 |
| 3.9.2.1 | Sensitization..... | 32 |
| 3.9.2.2 | Annealing..... | 32 |
| 3.10 | Preparation of Counter Electrode..... | 32 |
| 3.11 | Optical and Electrical Characteristics of Working Electrodes..... | 33 |
| 3.12 | Assembling of Dye Sensitized Solar Cell and Performance Evaluation... | 33 |
| 3.13 | I-V Characterization of DSSCs..... | 33 |
| CHAPTER FOUR | | |
| 4.0 | Results..... | 35 |
| CHAPTER FIVE | | |
| 5.1 | Conclusion.....,,..... | 54 |
| 5.2 | Recommendation for further study..... | 55 |
| | References..... | 56 |

LIST OF TABLES

| | | |
|--------------|--|----|
| Table 3.1: | Specification factors used in preparation of photoanode modified with silver nanoparticles..... | 31 |
| Table 4.1.4: | Shows optical characterization of each photoanode device..... | 45 |
| Table 4.2: | Performance characteristics of DSSCs fabricated with different anodes under 100mWcm..... | 49 |

LIST OF FIGURES

| | | |
|-------------|---|----|
| Figure 2.1: | Schematic of the layers of a typical PV cell..... | 15 |
| Figure 2.2: | The equivalent circuit of the solar cell..... | 16 |
| Figure 2.3: | Typical I-V characteristic of a crystalline silicon module with the variation of power..... | 17 |
| Figure 2.4: | I-V and P-V characteristics of solar cell module..... | 18 |
| Figure 2.5: | Dependency of the conversion efficiency on the semiconductor band gap | 20 |
| Figure 2.6: | The I-V characteristic of an ideal solar cell..... | 21 |
| Figure 3.1: | VWR ultrasonic cleaner and Spin-coater Machine from MSE, KWASU..... | 26 |
| Figure 3.2: | Carbolite tubular oven and single beam spectrophotometer Avantes from MSE, KWASU | 27 |
| Figure 3.3: | Scanning Electron Microscope from MSE, KWASU | 28 |
| Figure 3.4: | Circuit diagram for electrical characterization of the DSSCs..... | 34 |
| Figure 4.1: | The reflectance spectra of silver nanoparticles films, and the films annealed at different temperatures on glass substrates..... | 35 |
| Figure 4.2: | The transmittance spectra of silver nanoparticles films, and the films annealed at different temperatures on glass substrates..... | 36 |
| Figure 4.3: | The absorbance spectra of silver nanoparticles films, and the films annealed at different temperatures on glass substrates..... | 37 |
| Figure 4.4: | The bandgap spectra of silver nanoparticles films, and the films annealed at different temperatures on glass substrates..... | 38 |

| | | |
|--------------|--|----|
| Figure 4.5: | The reflectance spectra of mixed silver nanoparticles and TiO ₂ at different concentration films..... | 39 |
| Figure 4.6: | The transmittance spectra of mixed silver nanoparticles and TiO ₂ at different concentration films..... | 40 |
| Figure 4.7: | The reflectance spectra of mixed silver nanoparticles and TiO ₂ at different concentration films..... | 41 |
| Figure 4.8: | The bandgap spectra of mixed silver nanoparticles and TiO ₂ at different concentration films | 42 |
| Figure 4.9: | SEM image of silver nanoparticles not annealed and SEM image of silver nanoparticles annealed at (100-500) ⁰ C..... | 43 |
| Figure 4.10: | Current-voltage characteristics of the DSSC without silver nanoparticles..... | 46 |
| Figure 4.11: | Current-voltage characteristics of the DSSC with silver nanoparticles..... | 47 |
| Figure 4.12: | Current-voltage characteristics of the DSSC without silver nanoparticles..... | 48 |

CHAPTER ONE

INTRODUCTION

Solar radiation is the single most abundant energy source of our planet. For many millennia, humanity relied solely on renewable forms of solar energy making use of direct forms like lighting or heat, and indirect forms like biomass or wind. With the explosion of the world population at the beginning of the 20th century and its growing energy demand, humans started to tap fossil non-renewable forms of ancient biomass like oil, gas and coal extensively (Bagher *et al.*, 2015). Fossil energy sources possess a very high energy density and can be stored and transported easily seemingly a blessing for humanities energy needs.

We know now that our dependence on the burning of fossil fuels actually is a curse, which causes geopolitical tensions, environmental damage, and tragically puts our climate at stake. We clearly must move toward a more sustainable energy economy. Today, global primary energy is consumed at a rate of about 15 TW (McEvoy *et al.*, 2012), whereas our planet receives about 174×10^3 TW of solar radiation. Even if only a fraction of this energy can be harvested, the solar energy source is enormous and dwarfs all known non-renewable sources (McEvoy *et al.*, 2012).

The earth receives an incredible supply of solar energy. The sun, an average star, is a fusion reactor that has been burning over 4 billion years. It provides enough energy in one minute to supply the world's energy needs for one year. In one day, it provides more energy than our current population would consume in 27 years. In fact, the amount of solar radiation striking the earth over a three day period is equivalent to

the energy stored in all fossil energy sources." Solar energy is a free, inexhaustible resource, yet harnessing it is a relatively new idea (Bagher *et al.*, 2015).

Everyday sun sends out tremendous amount of energy in the form of heat and radiations called solar energy. Solar energy is a limitless source of energy which is available at no cost (Chu and Meisen, 2011; Choubey *et al.*, 2012). The major benefit of solar energy over other conventional power generators is that the sunlight can be directly harvested into solar energy with the use of small and tiny photovoltaic (PV) solar cells (McEvoy *et al.*, 2012).

A solar cell, or photovoltaic cell, is an electrical device that converts the energy of light directly into electricity by the photovoltaic effect, which is a combination of physical and chemical phenomenon (Eli *et al.*, 2016). It is a form of photoelectric cell, defined as a device whose electrical characteristics, such as current, voltage, or resistance, vary when exposed to light. Solar cells are the building blocks of photovoltaic modules, otherwise known as solar panels.

Dye Sensitized solar cells (DSSC), also sometimes referred to as dye sensitized cells (DSC), are a third generation photovoltaic (solar) cells that convert visible light into electrical energy. This new class of advanced solar cell can be likened to artificial photosynthesis due to the way in which it mimics nature's absorption of light energy. A dye sensitized solar cell (DSSC, DSC or DYSC) is a low-cost solar cell belonging to the group of thin film solar cells. (Bagher *et al.*, 2015). It is based on a semiconductor formed between a photo-sensitized anode and an electrolyte, a photo electrochemical system. (Bagher *et al.*, 2015).

1.2 Statement of the Problem

Dye sensitized solar cells (DSSC), is easy to manufacture, mostly low cost, and incorporate environmentally friendly materials. DSSC uses an organic dye to produce electricity in a wide range of light conditions, indoors and outdoors. However, there are certain challenges like degradation of dye molecules and hence stability issues. This is due to poor optical absorption of sensitizers which results in poor conversion efficiency. The dye molecules generally degrade after exposure to ultraviolet and infrared radiations leading to a decrease in the lifetime and stability of the cells. Moreover, coating with a barrier layer may also increase the manufacturing more expensive and lower the efficiency (Bagher *et al.*, 2015).

1.3 Justification of the Study

There is little or scanty information on the synthesis and characterization of silver nanoparticles to enhance dye sensitized solar cell. Eli *et al.*, (2016) reported an improved performance of a dye sensitized solar cell (DSSC) using silver nanoparticles (Ag-NPs) modified fluorine tin oxide (FTO) electrode through successive ion layer adsorption and reaction (SILAR). The resulting photo electrode was successfully incorporated in the DSSC with 22% improvement in photocurrent over the photocurrent (0.0259mAcm^{-2}) of bare FTO without Ag-NPs. Moreover, Saravanan *et al.*, (2017) also reported that the power conversion efficiency of the solar cell was improved from 2.83% to 3.62% after incorporation of the 2wt% of the silver nanoparticles. Maximum increases in open-circuit voltage (up to 12.1%) and in short-circuit current density (up to 10.7%) were observed. They used TiO_2 , AgNO_3 and extract from *Peltophorum pterocarpum* flowers to provide the plasmonic effect of green

synthesized silver nanoparticles. However, there was no report where *Carica papaya* leaves have been used as the source of dye in DSSC.

1.4 Aim of the Study

The aim of this study is to investigate the effect of green synthetic silver nanoparticles using *carica papaya* leaves for conversion efficiency enhancement of dye sensitized solar cells

1.5 Objectives of the Study

The objectives of this study are to:

- i. prepare silver nanoparticles using bio-synthesis method
- ii. characterize the structure of the synthesized nanostructured materials and study the optical properties of silver nanoparticles
- iii. study the interaction between working electrode and silver nanoparticles in relation to its performance efficiency
- iv. fabricate dye sensitized solar cells using Titanium dioxide/silver nanoparticles composite as photo anode.
- v. investigate the current-voltage properties of the fabricated DSSCs with silver nanoparticles modified photo anode and compare to one without silver nanoparticles.

1.6 Significance of Study

In the view of certain challenges like degradation of dye molecules and hence stability issues with DSSC due to poor optical absorption of sensitizers which results in poor conversion efficiency leading to reduction in the performance of the solar cell, it is hoped that the findings from this research would overcome these drawbacks and be significant in the following major areas: of Industry, Household and Research

1.7 Scope of Study

This project presents an overview of:

- i. Synthesis of silver nanoparticles
- ii. Characterization of silver nanoparticles
- iii. Fabrication of dye sensitized solar cell
- iv. Operating principle of dye sensitized solar cell
- v. Dye sensitized solar cell performance.

CHAPTER TWO

LITERATURE REVIEW

2.1 Solar Cells

The photovoltaic (PV) effect was first observed by Alexandre-Edmond Becquerel in 1839 (Yadav and Kumar, 2015). Subsequently, in 1946 the first modern solar cell made of silicon was invented by Russel Ohl (Castellano, 2010; Yadav and Kumar, 2015). Earlier photovoltaic solar cells are thin silicon wafers that transform sunlight energy into electrical power. The modern photovoltaic technology is based on the principle of electron hole creation in each cell composed of two different layers (p-type and n-type materials) of a semiconductor material. When a photon of sufficient energy impinges on the p-type and n-type junction, an electron is ejected by gaining energy from the striking photon and moves from one layer to another. This creates an electron and a hole in the process and by this process electrical power is generated (Srinivas *et al.*, 2015). The various types of materials applied for photovoltaic solar cells includes mainly in the form of silicon (single crystal, multi-crystalline, amorphous silicon) (McEvoy *et al.*, 2012), cadmium-telluride (McEvoy *et al.*, 2012), copper-indium-gallium-selenide (McEvoy *et al.*, 2012), and copper-indium-gallium-sulfide (Bagher *et al.*, 2015; Srinivas *et al.*, 2015). On the basis of these materials, the photovoltaic solar cells are categorized into various classes as follows.

2.2 First Generation Solar Cell-Wafer Based

The first generation solar cells are produced on silicon wafers. It is the oldest and the most popular technology due to high power efficiencies. The silicon wafer based technology is further categorized into two subgroups named as: Single/ Mono-

crystalline silicon solar cell and Poly/Multi-crystalline silicon solar cell (Choubey *et al.*, 2012; McEvoy *et al.*, 2012; Bagher *et al.*, 2015; Srinivas *et al.*, 2015).

2.2.1 Single/Mono-Crystalline Silicon Solar Cell

Mono crystalline solar cell, as the name indicates, is manufactured from single crystals of silicon by a process called Czochralski process (Srinivas *et al.*, 2015). During the manufacturing process, Si crystals are sliced from the big sized ingots. These large single crystal productions require precise processing as the process of “recrystallizing” the cell is more expensive and multi process. The efficiency of mono-crystalline single-crystalline silicon solar cells lies between 17% - 18% (Bertolli, 2008).

2.2.2 Polycrystalline Silicon Solar Cell (Poly-Si or Mc-Si)

Polycrystalline PV modules are generally composed of a number of different crystals, coupled to one another in a single cell. The processing of polycrystalline Si solar cells is more economical, which are produced by cooling graphite mold filled containing molten silicon. Polycrystalline Si solar cells are currently the most popular solar cells. They are believed to occupy most up to 48% of the solar cell production worldwide during 2008 (Saga, 2010). During solidification of the molten silicon, various crystal structures are formed. Though they are slightly cheaper to fabricate compared to mono-crystalline silicon solar panels, yet are less efficient ~12% - 14% (Jayakumar, 2009).

2.3. Second Generation Solar Cells-Thin Film Solar Cells

Most of the thin film solar cells and a-Si are second generation solar cells, and are more economical as compared to the first generation silicon wafer solar cells. Silicon-wafer cells have light absorbing layers up to 350 μm thick, while thin-film solar cells have a very thin light absorbing layer, generally of the order of 1 μm thickness

(Chopra *et al.*, 2004). Thin film solar cells are classified as; Amorphous Silicon Thin Film (A-Si), Cadmium Telluride (CdTe) Thin Film and Copper-indium-gallium diselenide (CIGS).

2.3.1 Amorphous Silicon Thin Film (a-Si) Solar Cell

Amorphous Si (a-Si) PV modules are the primitive solar cells that are first to be manufactured industrially. Amorphous (a-Si) solar cells can be manufactured at a low processing temperature, thereby permitting the use of various low cost, polymer and other flexible substrates. These substrates require a smaller amount of energy for processing (Imamzai *et al.*, 2012). Therefore, a-Si amorphous solar cell is comparatively cheaper and widely available. The “amorphous” word with respect to solar cell means that the comprising silicon material of the cell lacks a definite arrangement of atoms in the lattice, non-crystalline structure, or not highly structured. These are fabricated by coating the doped silicon material to the backside of the substrate/glass plate. These solar cells generally are dark brown in color on the reflecting side while silverish on the conducting side (Imamzai *et al.*, 2012).

The main issue of a-Si solar cell is the poor and almost unstable efficiency. The cell efficiency automatically falls at PV module level. Currently, the efficiencies of commercial PV modules vary in the range of 4% - 8%. They can be easily operated at elevated temperatures, and are suitable for the changing climatic conditions where sun shines for few hours (Maehlum, 2015).

2.3.2 Cadmium Telluride (CdTe) Thin Film Solar Cell

Among thin-film solar cells, cadmium telluride (CdTe) is one of the leading candidates for the development of cheaper, economically viable photovoltaic (PV) devices, and it is also the first PV technology at a low cost (Bertolli, 2008; Goswami

and Kreith, 2007; Luque and Hegedus, 2003). CdTe has a band gap of $\sim 1.5\text{eV}$ as well as high optical absorption coefficient and chemical stability. These properties make CdTe most attractive material for designing of thin-film solar cells.

CdTe is an excellent direct band gap crystalline compound semiconductor which makes the absorption of light easier and improves the efficiency. It is generally constructed by sandwiching between cadmium sulfide layers to form a p-n junction diode. The manufacturing process involves three steps: Firstly, the CdTe based solar cells are synthesized from polycrystalline materials and glass is chosen a substrate. Second process involves deposition, *i.e.*, the multiple layers of CdTe solar cells are coated on to substrate using different economical methods. It is already mentioned that CdTe has a direct optimum band gap ($\sim 1.45\text{eV}$) with high absorption coefficient over $5 \times 10^{15}/\text{cm}$ (Elsabawy *et al.*, 2012). Therefore, its efficiency usually operates in the range 9% -11% (Badawy, 2015). CdTe solar cells can be made on polymer substrates and flexible. However, there are various environmental issues with cadmium component of solar cell. Cadmium is regarded as a heavy metal and potential toxic agent that can accumulate in human bodies, animals and plants. The disposal of the toxic CdTe based materials as well as their recycling can be highly expensive and damaging too to our environment and society (Bagher *et al.*, 2015; Maehlum, 2015). Therefore, a limited supply of cadmium and environmental hazard associated with its use are the main issues with this CdTe technology (Sethi *et al.*, 2011; Elsabawy *et al.*, 2012; Badawy, 2015).

2.3.3 Copper Indium Gallium Di-Selenide (CIGS) Solar Cells

CIGS is a quaternary compound semiconductor comprising of the four elements, namely: Copper, Indium, Gallium and Selenium (Andorka, 2014; Bagher *et*

al., 2015). CIGS are also direct band gap type semiconductors. Compared to the CdTe thin film solar cell, CIGS hold a higher efficiency ~10% - 12%. Due to their significantly high efficiency and economy, CIGS based solar cell technology forms one of the most likely thin film technologies. The processing of CIGS is done by the following techniques: sputtering, evaporation, electrochemical coating technique, printing and electron beam deposition (Razykov *et al.*, 2011; Srinivas *et al.*, 2015). In addition, the sputtering can be a two or multi-step processes involving the deposition and subsequent interaction with selenium later, or can be a one-step reactive process. However, evaporation is similar to the sputtering in the sense that it can be used in a single step, two-step or multiple processing steps. The substrates for CIGS material can be chosen from glass plate, polymers substrates, steel, aluminum etc. The advantages of CIGS thin film solar cells include its prolonged life without a considerable degradation. These properties of CIGS indicate an easy solution to enhance the efficiency (Imamzai *et al.*, 2012; Badawy, 2015).

2.4 Third Generation Solar Cells

Third generation cells are the new promising technologies but are not commercially investigated in detail. Most of the developed third generation solar cell types are: Nanocrystal based solar cells, Polymer based solar cells, Dye sensitized solar cells and concentrated solar cells (Choubey *et al.*, 2012).

2.4.1 Nano Crystal Based Solar Cells

Nanocrystal based solar cells are generally also known as Quantum dots (QD) solar cells. These solar cells are composed of a semiconductor, generally from transition metal groups which are in the size of Nanocrystal range made of semiconducting materials. QD is just a name of the crystal size ranging typically within

a few nanometers in size, for example, materials like porous Si or porous TiO₂, which are frequently used in QD. With the advance of nanotechnology, these Nano crystals of semiconducting material are targeted to replace the semiconducting material in bulk state such as a-Si, CdTe or CIGS. This idea of the QD based solar cell with a theoretical formulation were employed for the design of a p-i-n solar cell over the self-organized in As/GaAs system (Hoppe and Sariciftci, 2008).

Generally, the nano crystals are mixed into a bath and coated onto the Si substrate. These crystals rotate very fast and flow away due to the centrifugal force. Generally, in conventional compound semiconductor solar cells, a photon will excite an electron there by creating one electron-hole pair (Dubey *et al.*, 2013). However, when a photon strikes a QD made of the similar semiconductor material, numerous electron-hole pairs can be formed, usually 2 or 3, also 7 has been observed in few cases (Sethi *et al.*, 2011; Choubey *et al.*, 2012)

2.4.2 Polymer Solar Cells

Polymer solar cells (PSC) are generally flexible solar cells due to the polymer substrate. The first PSC were invented by the research group of Tang *et al.* at Kodak Research Lab. (Choubey *et al.*, 2012). A PSC is composed of a serially connected thin functional layers coated on a polymer foil or ribbon. It works usually as a combination of donor (polymer) and a acceptor (fullerene). There are various types of materials for the absorption of sunlight, including organic material like a conjugate/conducting polymer (Choubey *et al.*, 2012; Ganesh and Supriya, 2013). In 2000, Heeger, MacDiarmid, and Shirakawa fetched the Nobel Prize in Chemistry for the discovering a new category of polymer materials known as conducting polymers (Leroy, 2003). The PSC and other organic solar cells operate on same principle known as the photovoltaic

effect, *i.e.*, where the transformation of the energy occurs in the form of electromagnetic radiations into electrical current (Alex *et al.*, 2007). Yu *et al.* mixed poly [2-methoxy-5-(2'-ethylhexyloxy)-p-phenylenevinylene] (PPV), C₆₀ and its other derivatives to develop the first polymer solar cell and obtained a high power conversion efficiency (Wudl and Srdanov, 1993). This process triggered the development of a new age in the polymer materials for capturing the solar power. After significantly optimizing the parameters, researchers achieved efficiency over 3.0% for PPV type PSCs (Li *et al.*, 2012). These unique properties of PSCs opened a new gateway for new applications in the formation of stretchable solar devices including textiles and fabrics (Li *et al.*, 2012). A modern recycling concept known as polarizing organic photovoltaic (ZOPVs) was also developed for increasing the function of liquid crystal displays utilizing the same polarizer, a photovoltaic device and proper light conditions/solar panel (Zhu *et al.*, 2011; Li *et al.*, 2012).

2.4.3 Dye Sensitized Solar Cells (DSSC)

Recent research has been focused on improving solar efficiency by molecular manipulation, use of nanotechnology for harvesting light energy ((Nozik, 2010; Graetzel *et al.*, 2012). The first DSSC solar cell was introduced by Michel Gratzel in Swiss federal institute of technology (Bagher *et al.*, 2015; Srinivas *et al.*, 2015). DSSCs based solar cells generally employ dye molecules between the different electrodes. The DSSC device consists of four components: semiconductor electrode (n-type TiO_2 and p-type NiO), a dye sensitizer, redox mediator, and a counter electrode (carbon or Pt) (Suhaimi *et al.*, 2015). The DSSC attractive due to the simple conventional processing methods like printing techniques, are highly flexible, transparent and low cost as well (Bagher *et al.*, 2015). The novelty in the DSSC solar cells arise due to the

photosensitization of Nanograined TiO₂ coatings coupled with the visible optically active dyes, thus increasing the efficiencies greater than 10% (Graetzel *et al.*, 2012; Suhaimi *et al.*, 2015). However, there are certain challenges like degradation of dye molecules and hence stability issues (Bagher *et al.*, 2015). This is due to poor optical absorption of sensitizers which results in poor conversion efficiency. The dye molecules generally degrade after exposure to ultraviolet and infrared radiations leading to a decrease in the lifetime and stability of the cells. Moreover, coating with a barrier layer may also increase the manufacturing more expensive and lower the efficiency (Bertolli, 2008).

2.4.4 Concentrated Solar Cells

Concentrating photovoltaic (CPV) has been established since the 1970s (Nozik, 2010; Philipps *et al.*, 2015). It is the newest technology in the solar cell research and development. The main principle of concentrated cells is to collect a large amount of solar energy onto a tiny region over the PV solar cell. The principle of this technology is based on optics, by using large mirrors and lens arrangement to focus sunlight rays onto a small region on the solar cell (Bertolli, 2008). The converging of the sunlight radiations thus produces a large amount of heat energy. This heat energy is further driven by a heat engine controlled by a power generator with integrated. CPVs have shown their promising nature in solar world (Mohanta *et al.*, 2015; Philipps *et al.*, 2015). It can be classified into low, medium, and high concentrated solar cells depending on the power of the lens systems (Philipps *et al.*, 2015). Concentrating photovoltaic technology have the following merits, such as solar cell efficiencies >40%, absence of any moving parts, no thermal mass, speedy response time and can be scalable to a range of sizes.

2.5 Perovskite Based Solar Cell

Perovskites are a class of compounds defined by the formula ABX_3 where X represents a halogen such as I^- , Br^- , Cl^- , and A and B are cations of different size. Perovskite solar cells are recent discovery among the solar cell research community and possess several advantages over conventional silicon and thin film based solar cells. Conventional Si based solar cells need expensive, multiple processing steps and require high temperatures ($>1000^\circ C$) and vacuum facilities (Ahn *et al.*, 2015; Casey, 2015). The perovskites based solar cells can have efficiency up to 31% (Shi *et al.*, 2015). It can be predicted that these perovskites may also play an important role in next-generation electric automobiles batteries, according to an interesting investigation recently performed by Volkswagen (Casey, 2015; Shi *et al.*, 2015). However, current issues with perovskite solar cells are their stability and durability. The material degrades over time, and hence a drop in overall efficiency. Therefore more research is needed to bring these cells into the market place.

2.6 Characterization of Solar Cells

Practically all photovoltaic devices incorporate a p-n junction in a semiconductor across which the photo voltage is developed. These devices are also known as solar cells. A cross-section through a typical solar cell is shown in Figure 2.1. The semiconductor material has to be able to absorb a large part of the solar spectrum. Dependent on the absorption properties of the material the light is absorbed in a region more or less close to the surface. When light quanta are absorbed, electron hole pairs are generated and if their recombination is prevented they can reach the junction where they are separated by an electric field (Goetzberger *et al.*, 2003). The photoelectric effect was first noted by a French physicist, Edmund Becquerel, in 1839, who found that

certain materials would produce small amounts of electric current when exposed to light. The theory of the solar cell is the solar effect of semiconductor material. The solar effect is a phenomenon that the semiconductor material absorbs the solar energy, and then the electron-hole excited by the photon separates and produces electromotive force.

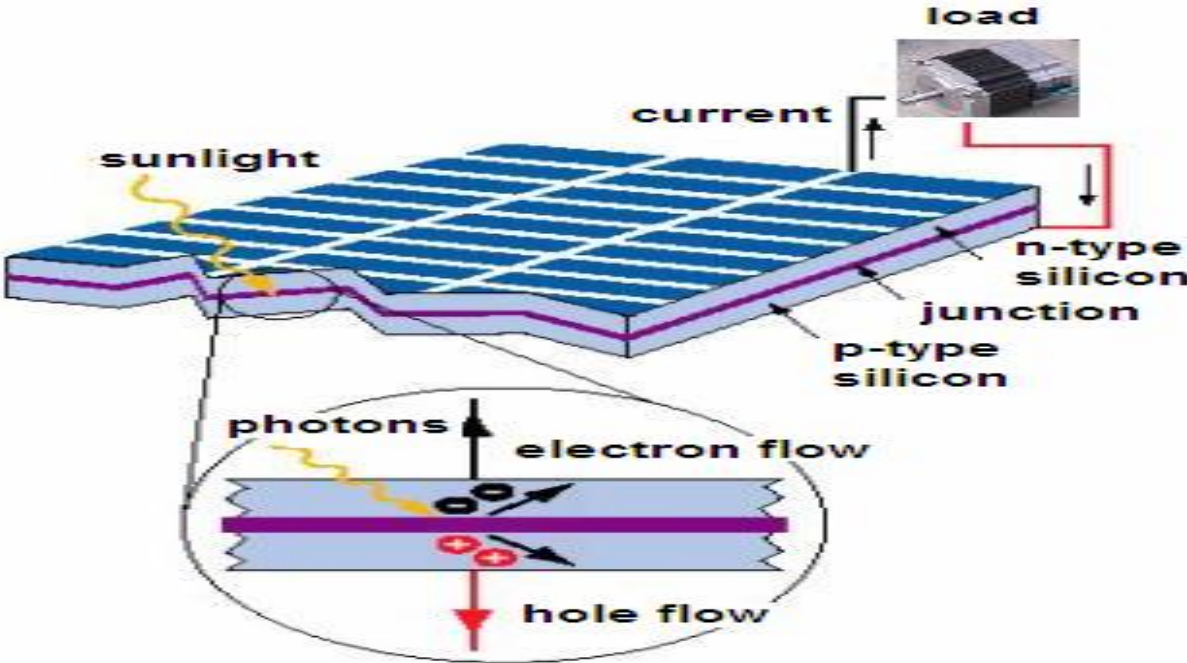


Figure 2.1: A schematic of the layers of a typical PV cell (Furkanand Mehmet, 2010).

The I-V characteristic of the solar cell changes with the sunshine intensity S (W/m^2) and cell temperature t ($^{\circ}C$), that is $I = f(V, S, t)$. According to the theory of electronics, when the load is pure resistance, the actual equivalent circuit of the solar cell is as Figure 2.2 (Ma *et al.*, 2009).

$I_{L\ Is}$ current supplied by solar cell.

$$I = I_L - I_0 \left[\exp \left(\frac{q(v + IR_s)}{AKT} \right) - 1 \right] \frac{v + IR_s}{R_{SH}} \dots \dots \dots (1)$$

Where, I_d , the junction current of the diode

$$I_d = I_0 \left[\exp \left(\frac{q(v + IR_s)}{AKT} \right) - 1 \right]$$

I , the load current

I_L , the photovoltaic current,

I_0 , the reverse saturation current

q , electronic charge,

k , Boltzmann constant,

T , absolute temperature, A , factor of the diode quality

R_s , series resistance,

R_{SH} , parallel resistance

Another important parameter is open circuit voltage

V_{oc} ;

$$V_{oc} = \frac{KT}{q} \ln \left(\frac{I_L}{I_0} + 1 \right) \approx \frac{KT}{q} \ln \left(\frac{I_L}{I_0} \right) \dots \dots \dots (2)$$

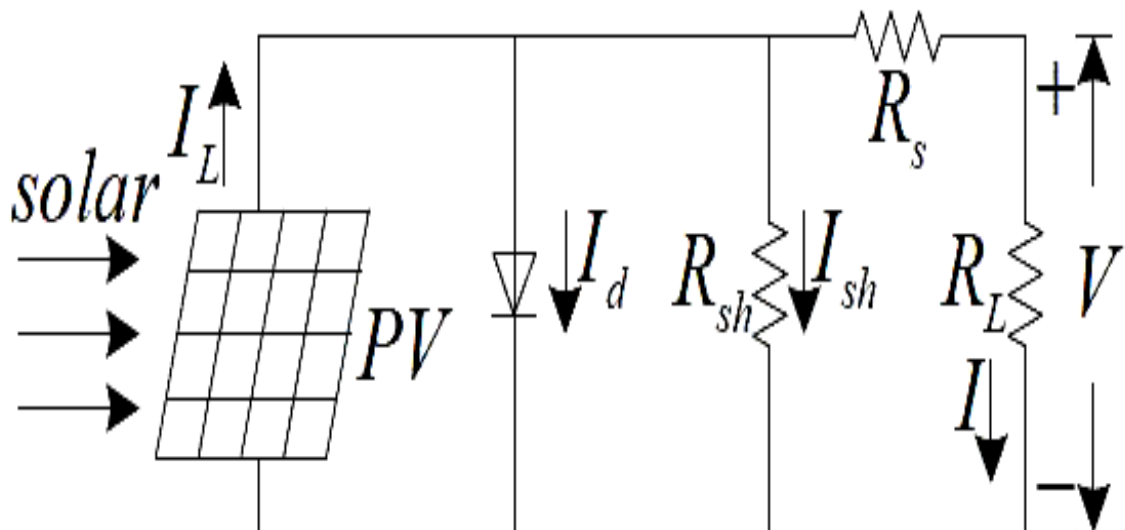


Figure 2.2: The equivalent circuit of the solar cell (Ma *et al.*, 2009).

Figure 2.3 shows an I-V characteristic together with the power curve, to illustrate the position of the maximum power point (Pearsall and Hill, 2002).

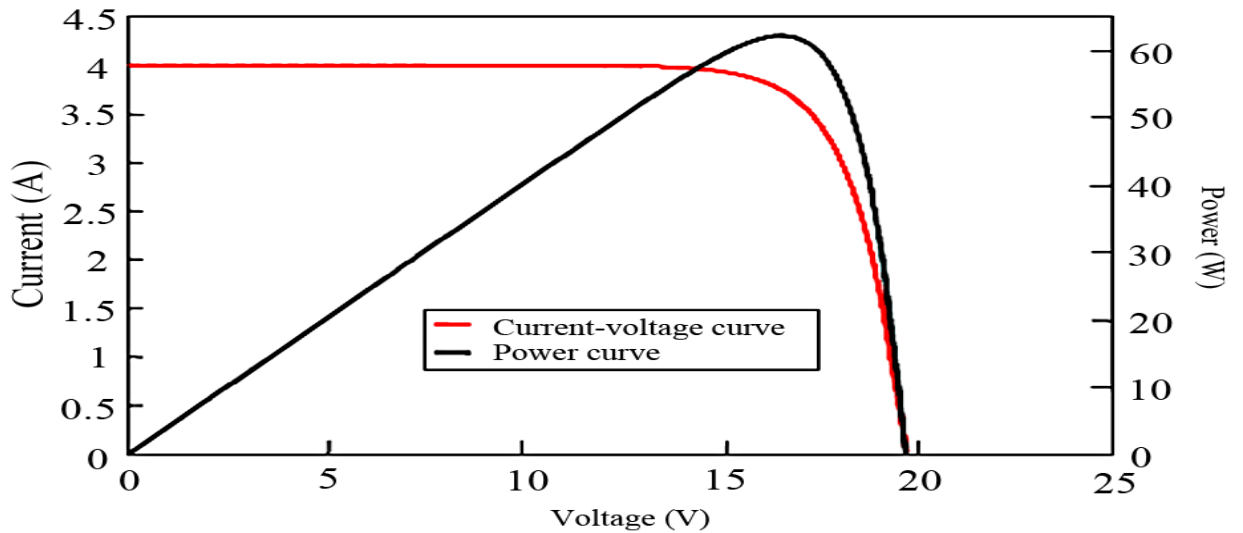


Figure 2.3. Typical I-V characteristic of a crystalline silicon module with the variation of power (Pearsall and Hill, 2002).

2.7 Solar Cells Efficiency

2.7.1 Cell Temperature

As temperature increases, the band gap of the intrinsic semiconductor shrinks, and the open circuit voltage (V_{oc}) decreases following the p-n junction voltage temperature dependency of seen in the diode factor $\frac{q}{KT}$. Solar cells therefore have a negative temperature coefficient of V_{oc} (β). Moreover, a lower output power results given the same photocurrent because the charge carriers are liberated at a lower potential. Using the convention introduced with the Fill Factor calculation, a reduction in V_{oc} results in a smaller theoretical maximum power $P_{max} = I_{sc} \times V_{oc}$ given the same short-circuit current I_{sc} (Furkanand Mehmet, 2010).

As temperature increases, again the band gap of the intrinsic semiconductor shrinks meaning more incident energy is absorbed because a greater percentage of the incident light has enough energy to raise charge carriers from the valence band to the conduction band. A larger photocurrent results; therefore, I_{sc} increases for a given

insolation, and solar cells have a positive temperature coefficient of $I_{sc}(\alpha)$ (Furkan and Mehmet, 2010).

Figure 2.4 shows the I-V and P-V characteristics at the constant illumination when the temperature changes (Suita and Tadakuma 2006). Temperature effects are the result of an inherent characteristic of crystalline silicon cell-based modules. They tend to produce higher voltage as the temperature drops and, conversely, to lose voltage in high temperatures. Any solar panel or system derating calculation must include adjustment for this temperature effect (Furkan and Mehmet, 2010).

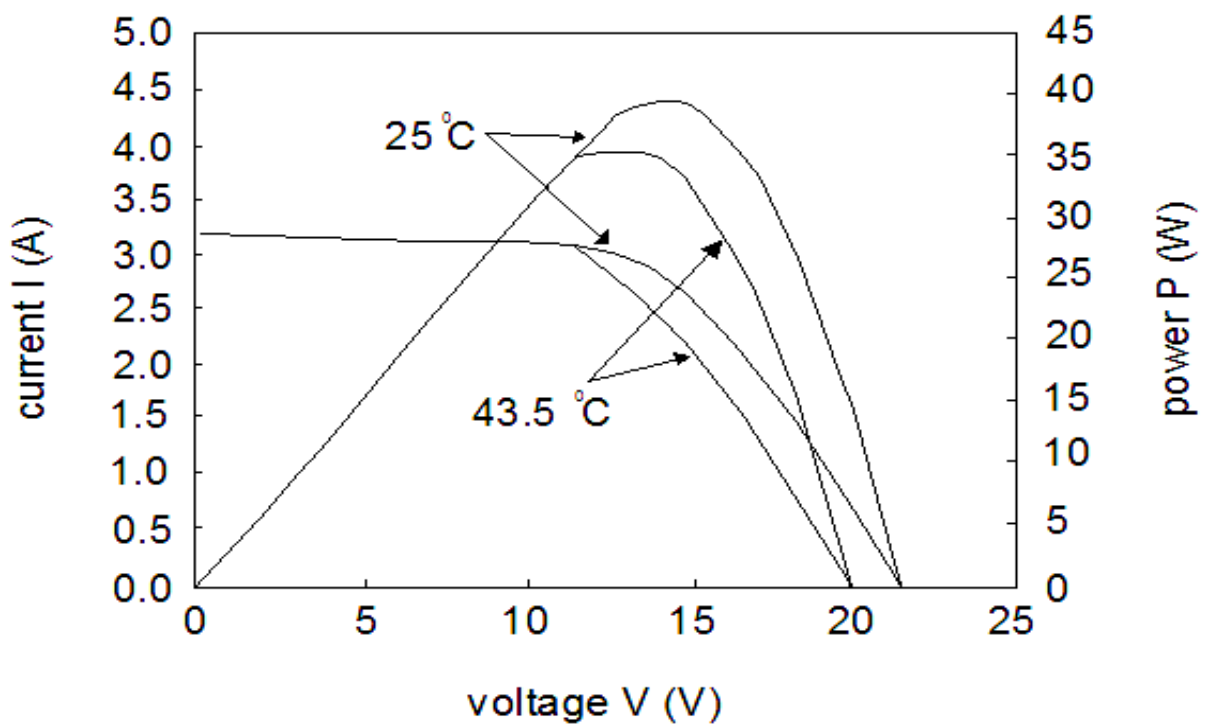


Figure 2.4. I-V and P-V characteristics of solar cell module (Suita and Tadakuma 2006).

2.7.2 Energy Conversion Efficiency

A solar cell's energy conversion efficiency (η , "eta"), is the percentage of power converted (from absorbed light to electrical energy) and collected, when a solar cell is connected to an electrical circuit. This term is calculated using the ratio of the maximum power point, P_m , divided by the input light irradiance (E , in W/m^2) under standard test conditions and the surface area of the solar cell (A_c in m^2) (Furkan and Mehmet, 2010).

$$\eta = \frac{P_m}{E \times A_c}$$

The efficiency of energy conversion is still low, thus requiring large areas for sufficient insulation and raising concern about unfavorable ratios of energies required for cell production versus energy collected (Queisser and Werner, 1995). In order to increase the energy conversion efficiency of the solar cell by reducing the reflection of incident light, two methods are widely used. One is reduction of the reflection of incident light with an antireflection coating, and the other is optical confinements of incident light with textured surfaces. They showed that the transformation of the wavelength of light could significantly enhance the spectral sensitivity of a silicon photodiode from the deep UV and through most of the visible region (Maruyama *et al.*, 1998).

The solar module has a different spectral response depending on the kind of the module. Therefore, the change of the spectral irradiance influences the solar power generation (Nishihata *et al.*, 2006). The solar spectrum can be approximated by a black body of 5900 K which results in a very broad spectrum ranging from the ultraviolet to the near infrared. A semiconductor, on the other hand can only convert photons with the energy of the band gap with good efficiency. Photons with lower energy are not

absorbed and those with higher energy are reduced to gap energy by thermalization of the photo generated carriers. Therefore, the curve of efficiency versus band gap goes through a maximum as seen from Figure 2.5 (Goetzberger *et al.*, 2003).

2.7.3 Maximum Power Point Tracking

Currently, the electricity transformation efficiency of the solar cells is very low that reach about 14%. The efficiency of solar cells should be improved with various methods. One of them is maximum power point tracking (MPPT) which is an important method. The MPPT operates with DC to DC high efficiency converter that presents an optimal and suitable output power. The resulting I-V characteristic is shown in Figure 2.5.

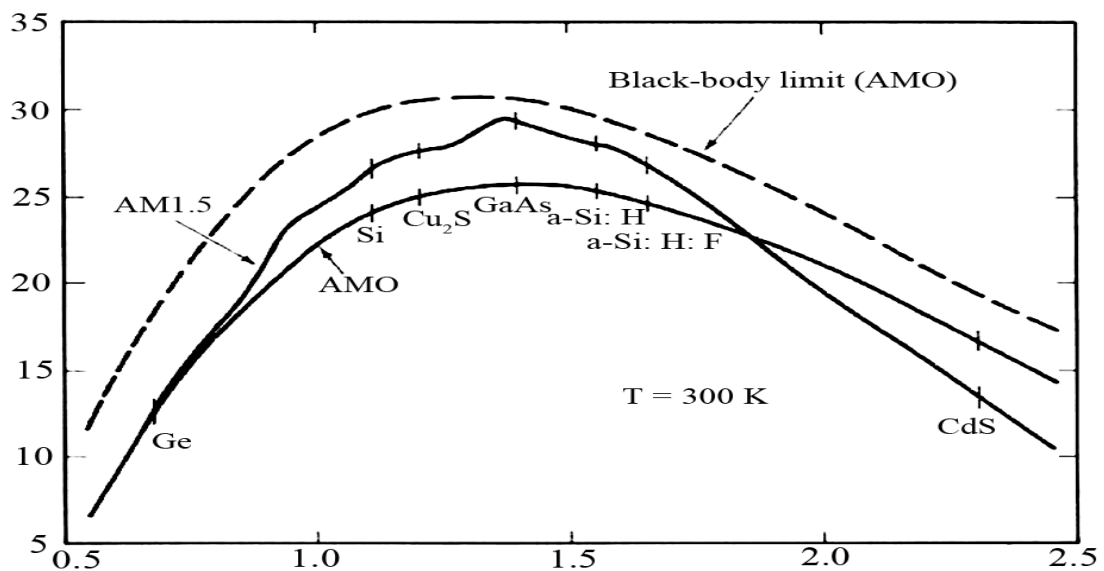


Figure 2.5. Dependency of the conversion efficiency on the semiconductor band gap (Furkan and Mehmet, 2010).

The photo generated current I_L is equal to the current produced by the cell at short circuit ($V = 0$). The open circuit Voltage V_{oc} (when $I = 0$) can easily be obtained as (Capar, 2005). No power is generated under short or open circuit. The maximum power

P produced by the conversion device is reached at a point on the characteristic. This is shown graphically in Figure 2.6

where the position of the maximum power point represents the largest area of the rectangle shown. One usually defines the fill-factor ff (Capar, 2005) by;

$$ff = \frac{P_{max}}{V_{oc} I_{sc}} = \frac{V_m I_m}{V_{oc} I_{sc}} \dots \dots \dots (4) \text{ where, } V_m \text{ and } I_m \text{ are the voltage and current at}$$

the maximum power point. When the output voltage of the photovoltaic cell array is very low, the output current changes little as the voltage changes, so the photovoltaic cell array is similar to the constant current source; when the Voltage is over a critical value and keeps rising, the current will fall sharply, now the photovoltaic cell array is similar to the constant voltage source.

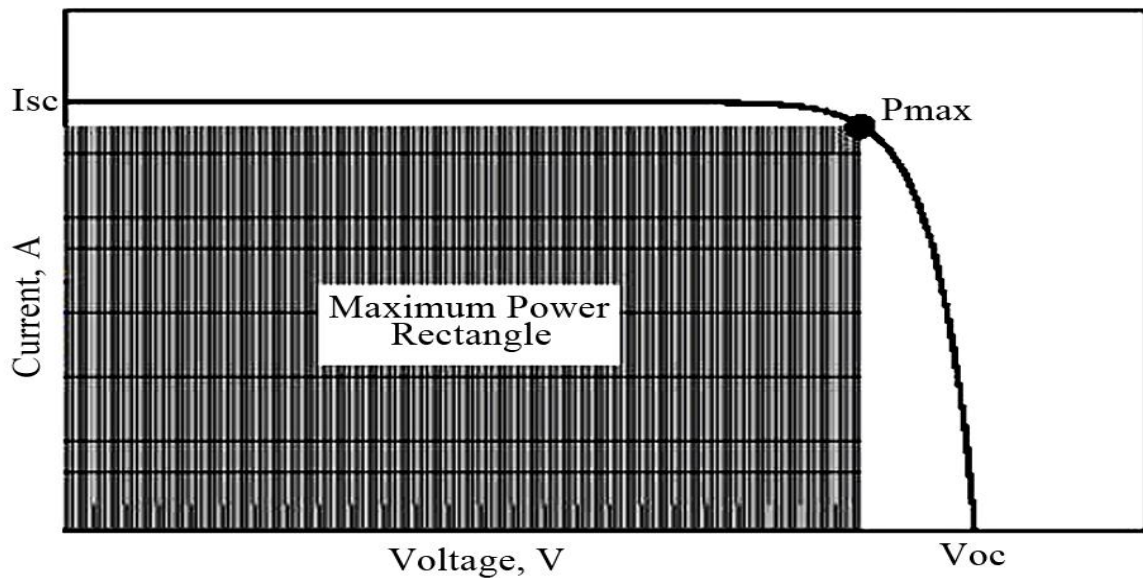


Figure 2.6. The I-V characteristic of an ideal solar cell (Capar, 2005).

As the output voltage keeps rising, the output power has a maximum power point. The function of the maximum power tracker is to change the equivalent load taken by the photovoltaic cell array, and adjust the working point of the photovoltaic cell

array, in order that the photovoltaic cell array can work on the maximum PowerPoint when the temperature and radiant intensity are both changing (Ma *et al.*, 2009).

2.8 Different Approaches of Some Related Research Works

In the last decade the processes and new materials for dye-sensitized solar cells (DSSCs) have been extensively researched in order to enhance the performance and the stability of the cells (Hagfeldt *et al.*, 2010; Asghar *et al.*, 2010; Berginc *et al.*, 2014). In order to broaden and/or increase the spectral sensitivity of the solar cell several concepts have been considered, for example, the quest for new sensitizers (Shi *et al.*, 2008; Wang *et al.*, 2003; Kuang *et al.*, 2007) or co sensitizers (Yella *et al.*, 2011; Zhang *et al.*, 2013; Lin *et al.*, 2014; Qin *et al.*, 2013), different approaches for engineering active layer/electrolyte interface (Zhang *et al.*, 2014), optimizing the thickness of the active layer, or increasing the concentration of the attached dye molecules (Ito *et al.*, 2006; Wang *et al.*, 2004). Absorption has also been improved by increasing the optical path using larger scattering particles or voids in the active layer (Wang *et al.*, 2004; Tachibana *et al.*, 2002; Nazeeruddin *et al.*, 2001). Furthermore, an undyed layer placed on top of the active layer (Ito *et al.*, 2006; Wang *et al.*, 2004; Horse *et al.*, 2006; Koo *et al.*, 2008) or a mirror-like Pt counter electrode (Fang *et al.*, 2004; Li *et al.*, 2007; Gratzel *et al.*, 2001) was studied as an internal back reflector. In addition, different materials have also been proposed as external back reflectors placed at the rear side of the DSSCs (Berginc, 2007).

Also, a surface plasmon resonance using metal nanoparticles (NPs) has also attracted much attention and has been studied for various solar cell technologies (Temple, *et al.*, 2009; Pillai and Green, 2010; Catchpole and Polman, 2008; Atwater

and Polman, 2010; Noguez, 2007). The surface Plasmon resonance is a light induced coherent oscillation of conduction band electrons on the surface of the metal NPs. The wavelength of resonance peak due to the presence of plasmonic particles greatly depends on factors such as size, shape, and dielectric environment. Two types of enhanced absorption are possible: (1) near-field: a strong electromagnetic field in the vicinity of the NPs around the plasmonic resonance wavelengths greatly enhances the absorption in the active layer and (2) far-field enhancement of the light absorption in the photoactive layer due to the scattering effect.

Efforts for achieving higher efficiencies are focused in optimizing the morphology of the active photovoltaic layer and the charge transport properties of the absorber through thermal annealing treatment (Ma *et al.*, 2005 ; Li *et al.*, 2005), use of various solvents (Dang *et al.*, 2011), the use of additives (Lee *et al.*, 2008). Alternatively, introduction of metallic nanoparticles (NPs) in suitable places to trap or confine light inside the active layer and enhance the absorption in the organic semiconductor film could provide superior performances (Westphalen *et al.*, 2000; Agglund *et al.*, 2008; Stenzel *et al.*, 1995; Chen *et al.*, 2008; Zhu *et al.*, 2011). Metal NPs embedded in a dielectric matrix strongly interact with light at their dipole surface Plasmon frequency due to the excitation of a collective electron motion (a so called Plasmon) inside the metal particle (Kreibig and Vollmer 1994). The surface confines the conduction electrons inside the particle and sets up an effective restoring force leading to resonant behavior at the dipole

Surface Plasmon frequency, namely Surface Plasmon Resonance (SPR). This resonance depends strongly on the shape, size and distribution of the NPs as well as on the dielectric functions of the metal and the dielectric surrounding environment.

Therefore, the line shape of the SPR can be widely tailored. Among the metals that support SPR modes, noble metals, gold, silver and copper (Au, Ag, Cu) exhibit resonances in the visible or near infrared region of the electromagnetic spectrum, which is the range of interest for photovoltaic applications. Researchers have designed and tested various plasmonic light-trapping geometries for enhancing conversion efficiency of DSSCs (Cole and Halas 2006; Lagos *et al.*, 2011), however, the interaction and working mechanisms in plasmonic DSSCs containing metal nanostructures are dramatically complicated. However, a detailed description of the kinetics of electrochemical and photo electrochemical processes in plasmonic DSSCs have not been established (Dingwen *et al.*, 2013).

CHAPTER THREE

MATERIALS AND METHODOLOGY

3.1 Materials

Materials used are Silver nitrate (AgNO_3), *carica papaya* leaf, deionized water, ethanol, isopropanol (IPA), glass substrate, fluorine-doped conducting glass (FTO), titanium dioxide (TiO_2) binder clips were used for the research.

3.2 Equipment

VWR ultrasonic cleaner with Digital Timer and heater 97043-986, Spin –coater model laurel WS-650Hz-23NPP, Carbolite tubular oven model Srw 21-501042 Type-CT17, single beam spectrophotometer Avantes model Avalight-DH-5-BAL, Scanning Electron Microscope (SEM) model ASPEX 3020 (Figures 3.1a&b, 3.2a&b and 3.3) were also used for the research.



Figure 3.1(a) VWR ultrasonic cleaner (b) Spin-coater Machine from MSE, KWASU.



Figure 3.2(a) Carbolite tubular oven (b) Single beam spectrophotometer Avantes from MSE, KWASU.



Figure 3.3. Scanning Electron Microscope (SEM) from MSE, KWASU

3.3 Synthesis of Silver Nanoparticles

Three grams of carica papaya leaves were thoroughly rinsed, cut into smaller piece then immersed in 300 mL of boiling distilled water for 30 min and then filtered. The obtained extract was dripped into 100 mL of 0.01 M aqueous silver nitrate solution with constant gentle stirring. The yellowish brown appearance of the product indicated the formation of the silver nanoparticles, it was then stored in a brown bottle.

3.4 Substrate Purification

Glass substrate of dimensions 25.4mm by 76.2mm was rinsed in de-ionized (DI) water. They were then placed in a beaker containing isopropanol (IPA) before cleaning in VWR ultrasonic cleaner with Digital Timer and heater 97043-986 at room temperature for 30 min. The cleaned glass substrates were dipped in ethanol and dried in a stream of nitrogen gas (N_2). All glass substrate received the same cleaning process.

3.5 Preparation of Silver Nanoparticles Thin Film

Thin films were obtained by spin coating the silver nanoparticles dropped onto the cleaned glass substrate placed on the stub of the spin-coater model laurel WS-650Hz-23NPP which was rotated at 3000 rpm for 30 sec at room temperature. After depositing by spin coating, the films were annealed at different temperatures ranging from 100°C to 500°C for 1hr with carbolite tubular oven model Srw 21-501042 Type-CT17 and allowed to cool to room temperature in an argon environment. One sample that was not subjected to heat treatment served as control.

3.6 Preparation of Silver Nanoparticles and TiO₂ Composite Thin Film

23wt% of TiO₂ in ethanol was stirred with magnetic stirrer at 90°C for 40 minutes. The thin film was prepared by depositing the glass substrate with mixed silver Nanoparticles and TiO₂. The green synthesized silver nanoparticles were mixed with

TiO₂ nanoparticles in different concentration in ratio 1:2, 5:8, 3:8, 1:4, 1:8 respectively. The obtained mixed silver nanoparticles with TiO₂ paste was spin coated on the glass substrate using the spin-coater model laurel WS-650Hz-23NPP. Which was rotated at 3000 rpm for 30 sec at room temperature. One sample that was not mixed with silver nanoparticles served as control.

3.7 Characterization of Structure and Optical Properties of Silver Nanoparticles

Surface morphology of thin film was studied using Scanning Electron Microscope (SEM) model ASPEX 3020. The optical absorbance and transmittance measurements were recorded by using a single beam spectrophotometer Avantes model Avalight-DH-5-BAL.

The absorption spectrum was recorded through double beam UV-VIS absorption spectrometer in the range of 100-1000 nm

3.8 Preparation of Conductive Glasses (FTO)

Cleaning of Substrates

- a). Cut FTO coated glass into a dimension of 25 x 25 cm².
- b). Wash the glass Substrate with detergent solution for 10 to 15 minutes.
- c). Rinse the substrate with distilled water in Ultrasonic bath for 15 minutes.
- d). Clean the substrate with IPA in ultrasonic bath for 15 minutes.
- e). Blow-dry the substrates with Nitrogen gas.

Liquid soap removes oily stain plus debris. Acetone removes organic forts and water molecules from the glass; methanol removes more water and acetone remnants, IPA removes left over water.

3.9 Preparation of Working Electrode (Anode)

The conductive side of glass was determined in the model kit by touching both of protruding leads of the multi-meter with one side of the glass. The conductive side was identified with average resistance from 20-38 ohms. The titanium dioxide paste was prepared by adding a few drops of ethanol (10.00mL) to 2.30 gram TiO₂. The resulting mixture was stirred with magnetic stirrer at 90⁰C for 40 minutes. The thickness of TiO₂ in this work was controlled by the tape thickness. Thus, by layering several pieces of tape on one side of the glass. 2-3 drops of the TiO₂ suspension added onto the conductive side and spread out the TiO₂ evenly on the surface of the plate with glass rod. Carefully remove the tape without perturbing the TiO₂ layer. The glass with TiO₂ dried under room temperature over 4 hours and then heat to 420 ⁰C for another 20 min, until the dried TiO₂ turns brown and then white again. In preparing the working electrode for each of the specimen used, the Tables 3.1 used as the specification factors.

Table 3.1: Specification Factors Used In Preparation Of Photo Anode Modified With Silver Nanoparticles.

| Sample | Thickness (nm) | Dye loading Time(Hours) | Annealing Temperature °C |
|--------|----------------|-------------------------|--------------------------|
| A | 96.981 | 6.00 | 80 |
| B | 214.143 | 12.00 | 160 |
| C | 378.704 | 18.00 | 240 |
| D | 414.458 | 24.00 | 320 |
| E | 462.187 | 30.00 | 400 |
| F | 499.123 | 36.00 | 480 |

3.9.1 Determination of Thickness of the Film

Assuming uniform deposition, hence uniform film thickness during deposition, the thickness of Tin (II) oxide films were determined by Equation 3.1

$$t = \frac{M_2 - M_1}{AD} \quad 3.1$$

M_1 = mass of substrate before deposition

M_2 = mass of substrate after deposition

A = Area covered by the film

D = Density of the SnO thin film (6.446g/cm³)

$$\text{Density} = \frac{m}{V} = \frac{M}{L^3} = \frac{m}{L^2 \times L}$$

$$AL = \frac{m}{\rho} \quad ; \quad L = \frac{m}{\rho A}$$

3.9.2 Dye Loading Time

3.9.2.1 Sensitization

For absorption on TiO₂, the FTO/TiO₂ slides were individually equilibrated in the respective dye solution for hours specified in Table 3.1 for sensitization, after which the slide was immediately washed with excess ethanol and dried in gentle nitrogen flow to remove any water content.

After the specified time, the specimens were carefully removed; air dried and kept in a sealed petridishes. The outer surfaces of the petridishes were covered with black tape to prevent the specimen from direct sunlight. The Electrolube silver conductive paint was applied to the conductive side for better interface conductivity.

The sample of sensitizers were then prepared as specified in the Table 3.1

3.9.2.2 Annealing

The specimens were annealed with electric oven set at different temperatures and for duration specified in the Table 3.1 and allowed to cool. They were then kept in well covered glassware to prevent contamination.

3.10 Preparation of Counter Electrode.

To prepare the counter electrode using carbon, the FTO glass was wiped with ethanol. Then, the FTO glass surface was colored by using graphite carbon pencil. After that, the surface was checked to ensure that there was no space that the carbon did not cover

3.11 Optical and Electrical Characteristics of Working Electrodes

The average transmittance and absorbance values in the visible light region (400nm – 700nm) for each of the samples were determined from the graphs of absorbance and transmittance spectrum. Measurements of sheet resistance of each of the samples were carried out using four point probe technique. The plots of the each of samples were carried out and the optical band gap of the sample were determined from the plots.

3.12 Assembling of Dye Sensitized Solar Cell and Performance Evaluation

The cathode electrode and the anode electrode were put together, overlapping each other, and a space at the end of each electrode was made. Next, both electrodes were fasten using the double clip. Three drops of iodide solution were added in the space existing between the anode layer and counter anode at the end of the electrode and the solutions were spread over the entire electrode. Then, the remaining iodide solution was wiped off using cotton swab soaked with alcohol. After that, a tester with

crocodile clip was attached at both ends of the electrode. The experiment was conducted under the halogen lamp (110V, 250W).

3.13 I-V Characterization of DSSCs

The I-V characterization of the DSSCs was carried out under constant illumination of 28.282mW/cm² with a Xenon lamp. By series connection of each of the fabricated DSSC in series to a tunable resistor (100-1000 Ω) and connecting a voltmeter in parallel as shown in Figure 3.4. The voltages read from the voltmeter and the current calculated using Ohm`s law plotted to obtain the I-V characteristics curves from which the maximum voltage V_m and maximum current I_m open circuit voltage V_{oc} and short circuit current I_{sc} were obtained for each of the cells. The overall conversion efficiencies and fill factors were calculated using eqn 3.3 and eqn 3.2 respectively:

$$\text{Fill Factor } FF = \frac{I_m \times V_m}{I_{sc} \times V_{oc}} \quad 3.2$$

$$\text{Efficiency} = \frac{I_m \times V_m}{\text{Input Photon Power}} \times 100\% = \frac{I_{sc} \times V_{oc} \times FF}{\text{Input Photon Power}} \times 100\% \quad 3.3$$

The input photon power was obtained by multiplying the measured light intensity with the active cell area. The shunt resistance which is the inverse of the slope at I_{sc} and the series resistance which is at least proportional to the inverse of the slope of the I-V curve at V_{oc} were also estimated for each solar cell.

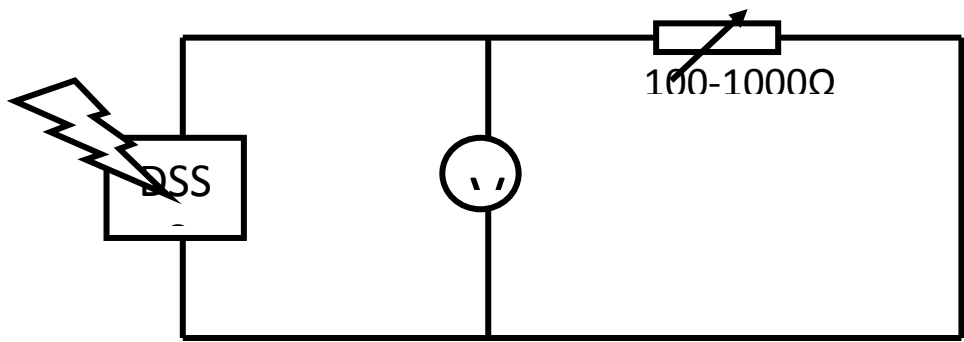


Figure 3.4: Circuit Diagram for Electrical Characterization of the DSSCs

CHAPTER FOUR
RESULTS AND DISCUSSION

4.0 Results

4.1 Characterization of structure and optical properties of Silver Nanoparticles

Reflectance Spectra

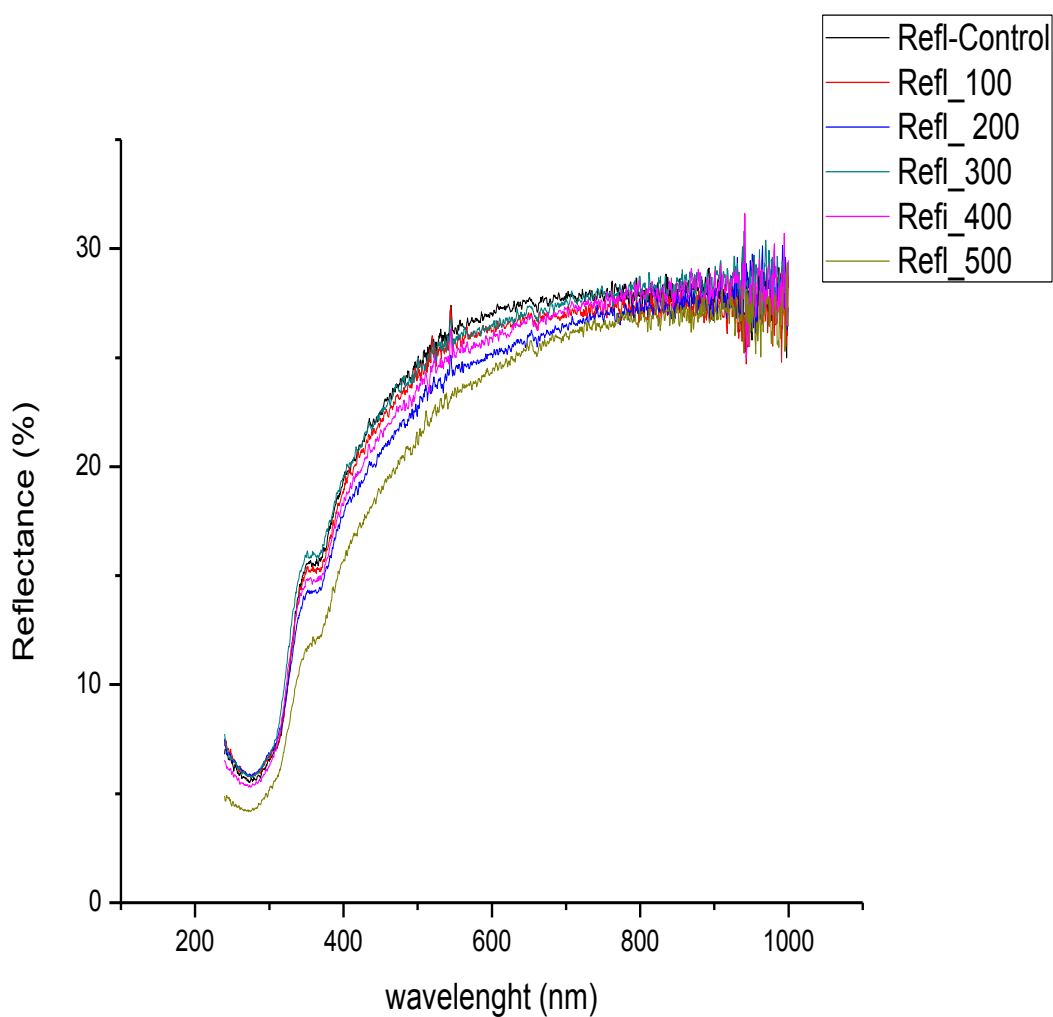


Figure 4.1: The reflectance spectra of silver nanoparticles films, and the films annealed at different temperatures on glass substrates, Refl= reflectance spectra.

Transmittance Spectra

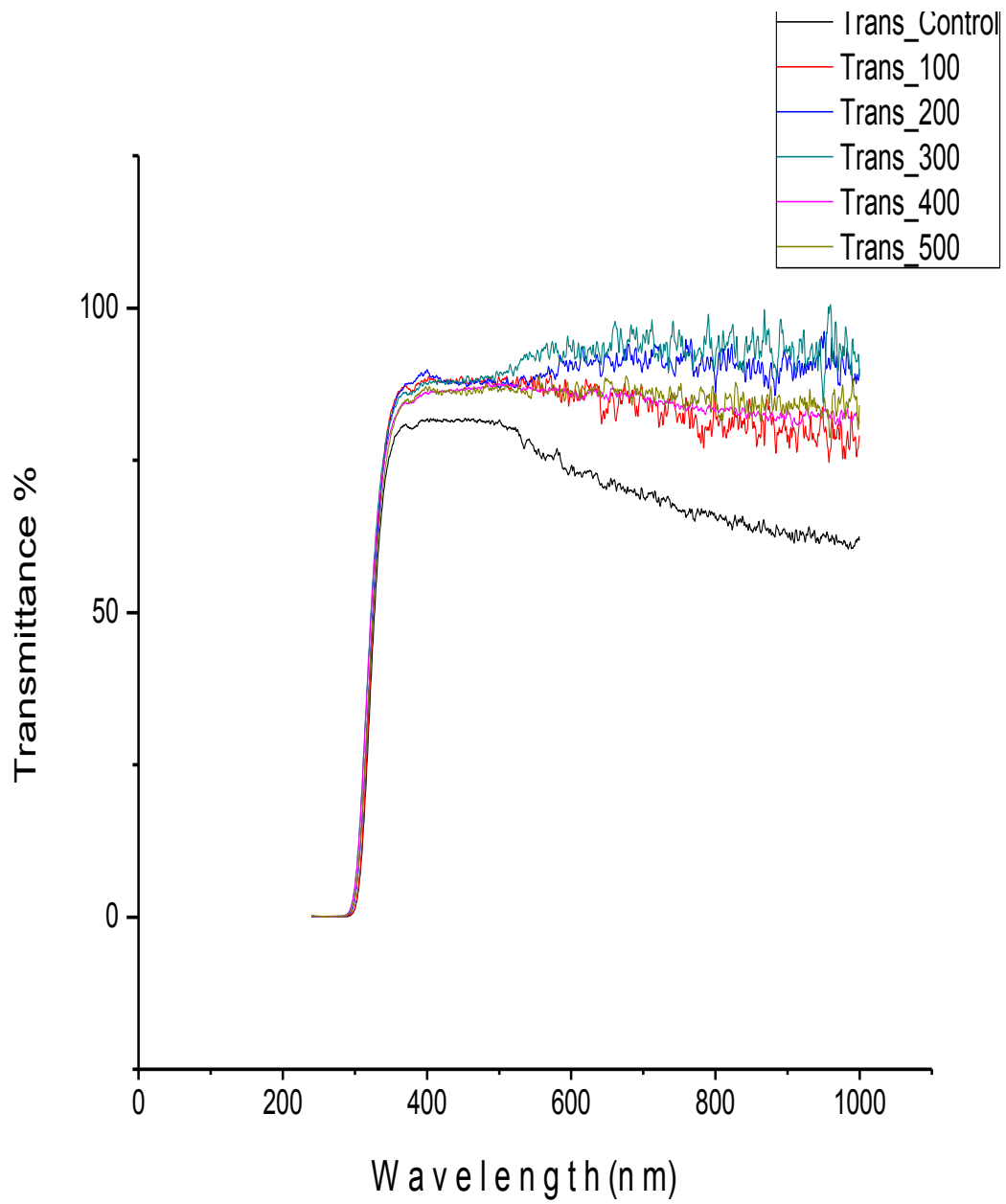


Fig.4.2: The transmittance spectra of silver nanoparticles films, and the films annealed at different temperatures on glass substrates, Trans= transmittance spectra.

Absorption Spectra

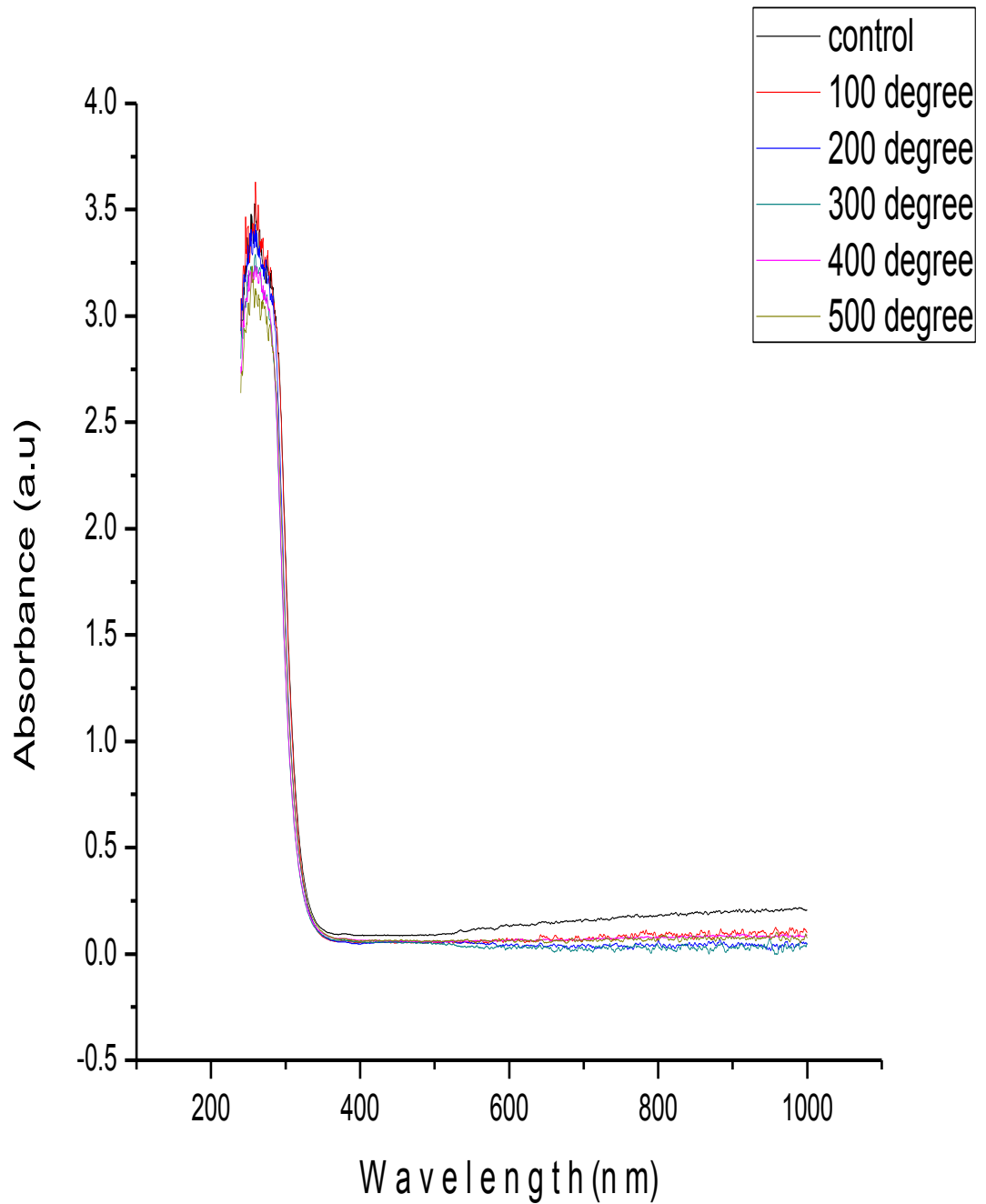


Fig. 4.3: The absorbance spectra of silver nanoparticles films, and the films annealed at different temperatures on glass substrates.

Bandgap Spectra

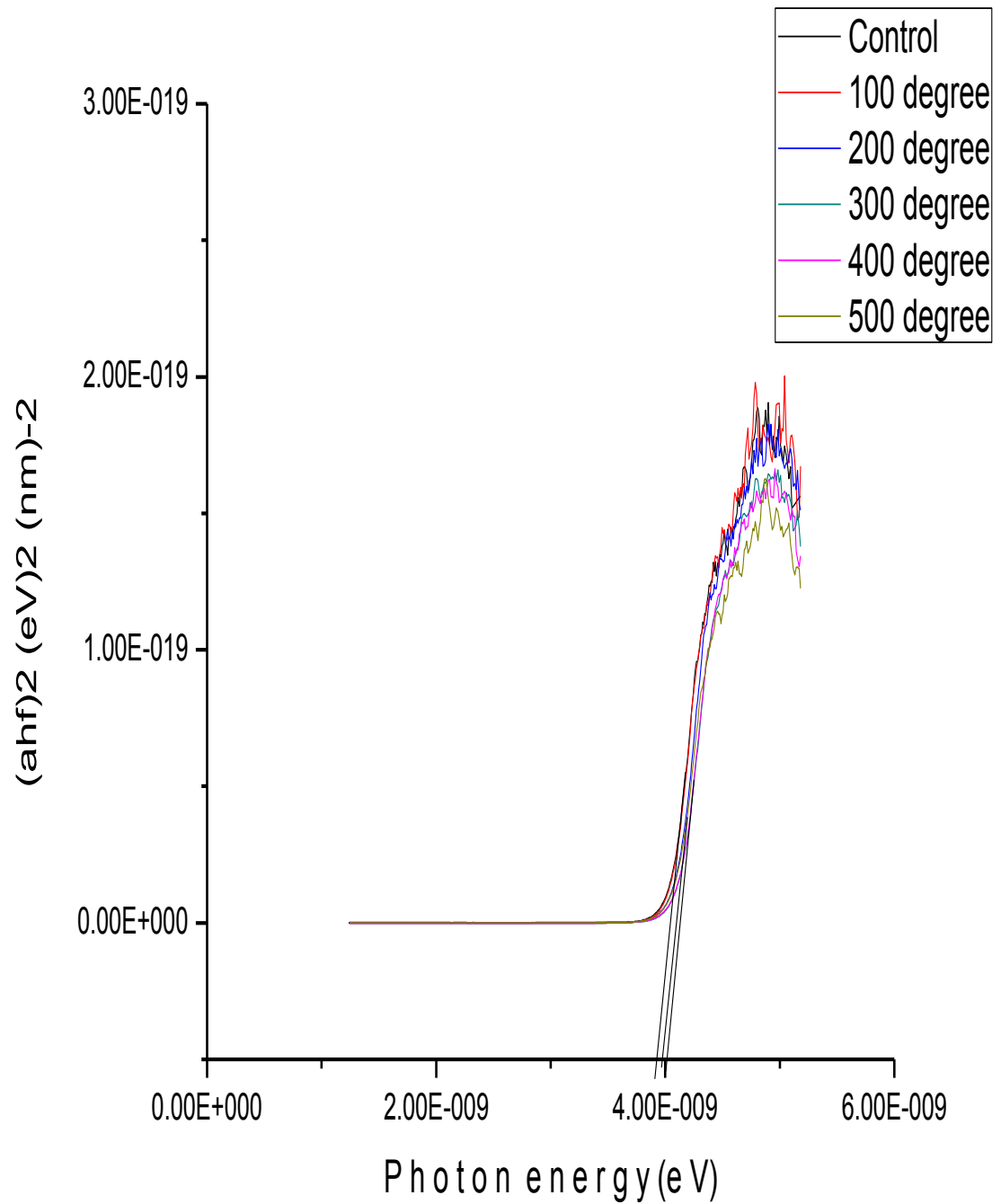


Fig.4.4: The bandgap spectra of silver nanoparticles films, and the films annealed at different temperatures on glass substrates.

4.2 Optical Properties of Silver Nanoparticles/Titanium oxide Thin Film

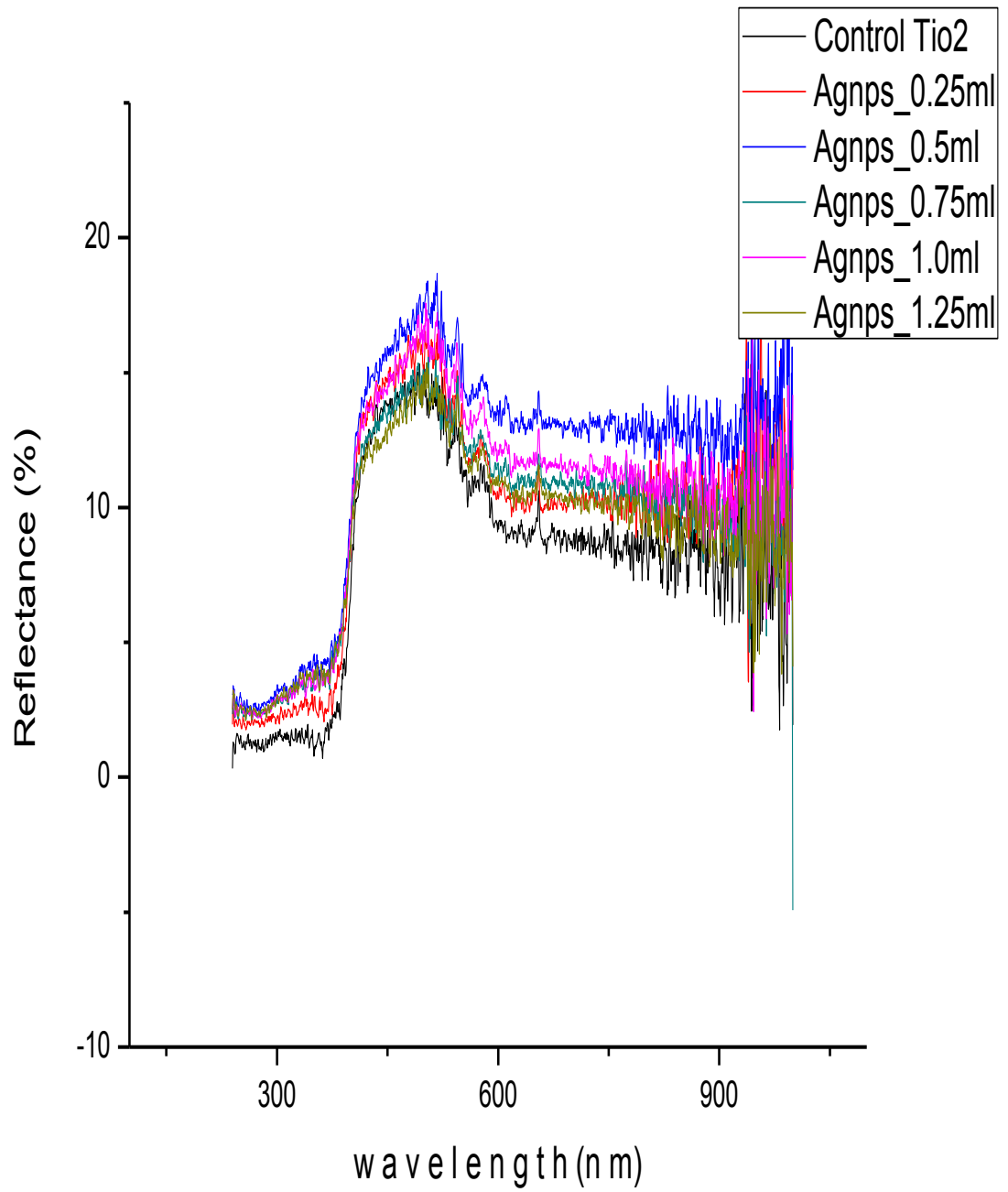


Fig. 4.5: The Reflectance spectra of mixed silver nanoparticles and TiO_2 at different concentration films.

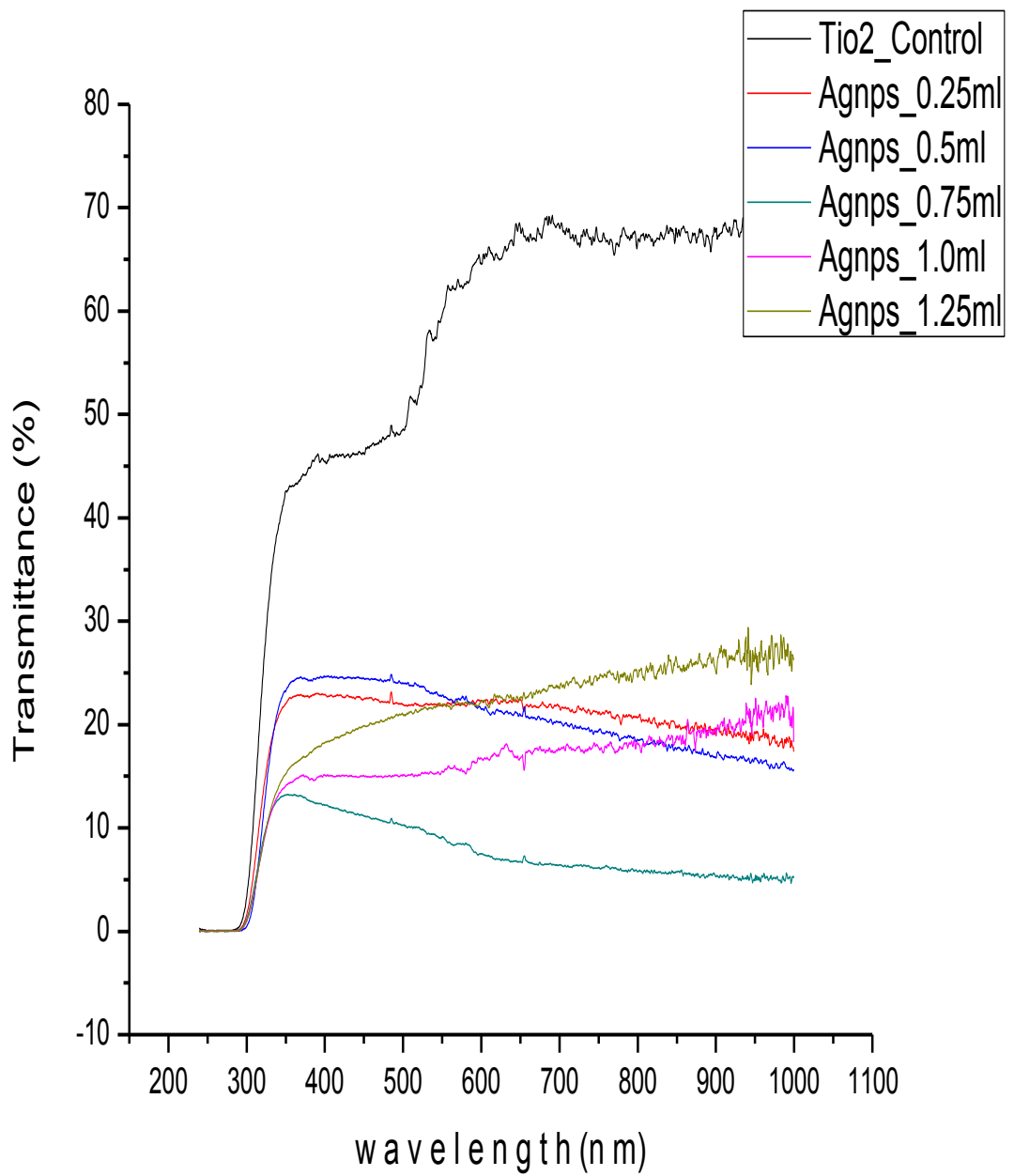


Fig.4.6: The transmittance spectra of mixed silver nanoparticles and TiO₂ at different concentration films.

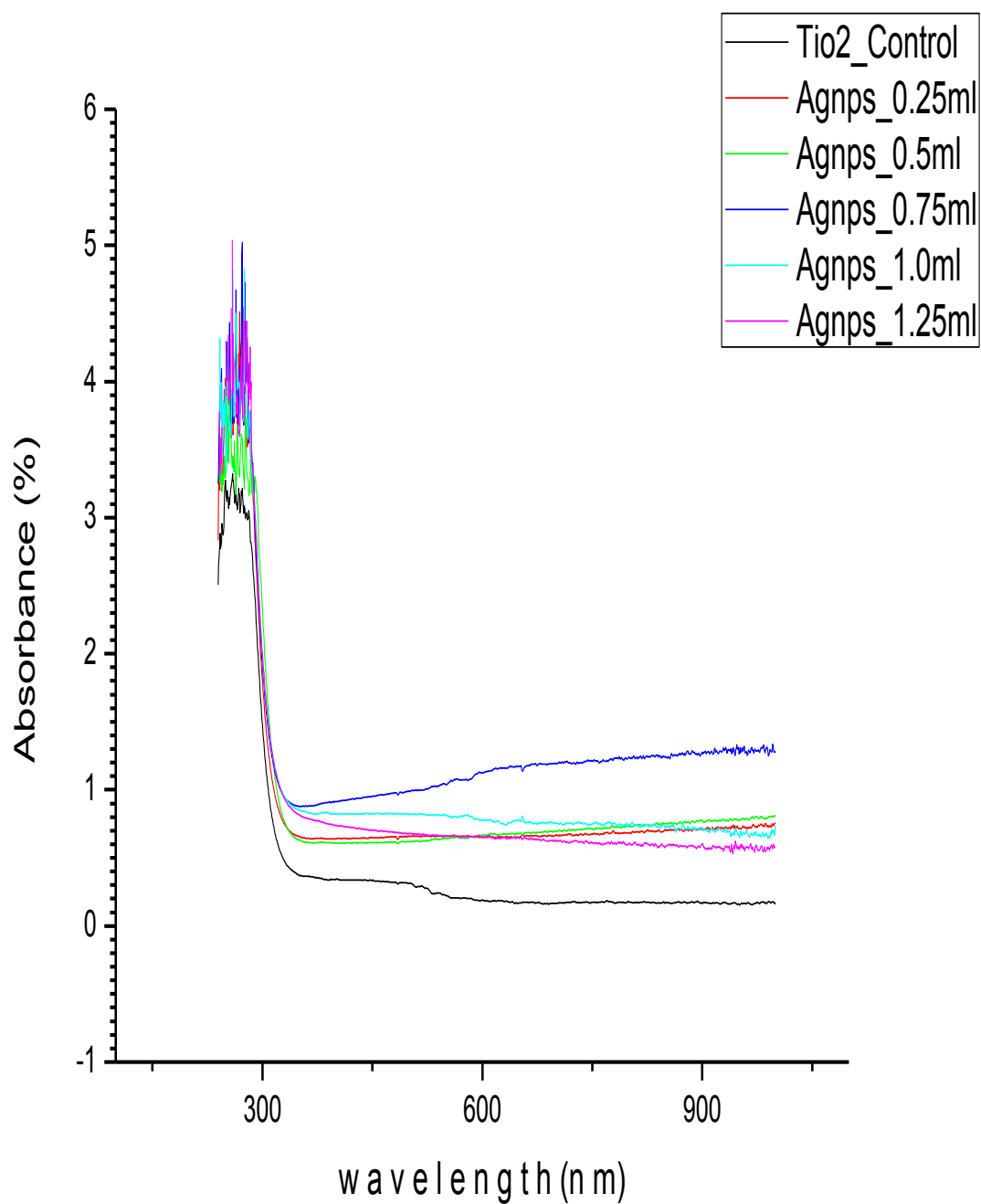


Fig.4.7: The absorbance spectra of mixed silver nanoparticles and TiO₂ at different concentration films.

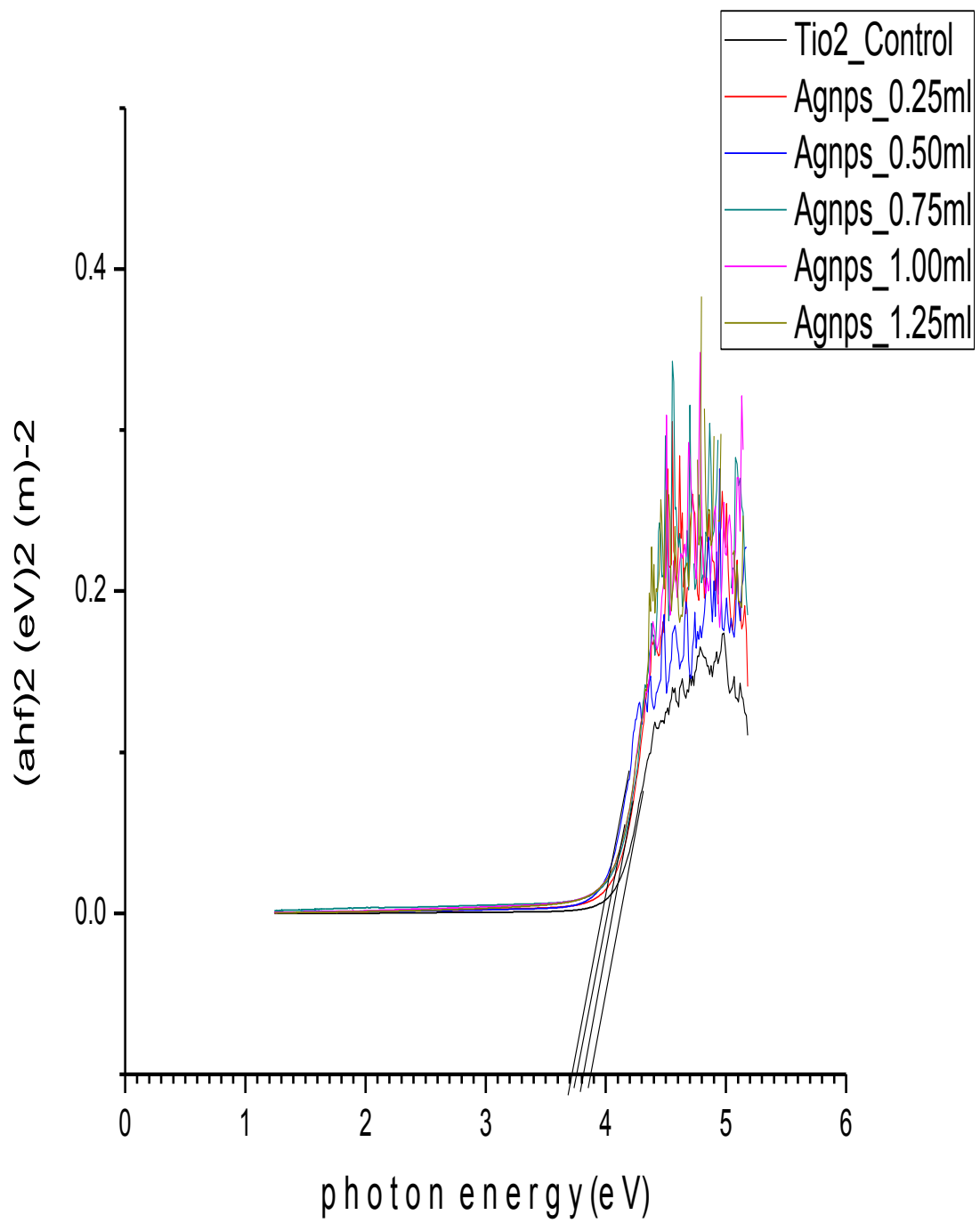


Figure 4.8: The bandgap spectra of mixed silver nanoparticles and TiO₂ at different concentration films, AgNPs= silver nanoparticles.

4.3 Morphological Characterization

Figures 4.9 a-f show SEM images of silver nanoparticles deposited on glass substrate and annealed at different annealing temperatures and a film which was not annealed. The surface of silver nanoparticles without annealing was relatively smooth. A few holes have appeared after annealing from 100°C - 500°C , the roughness of the surface of the sample increased as annealing temperature increased. The results showed that annealing temperature significantly influenced the size and shape of silver particles.

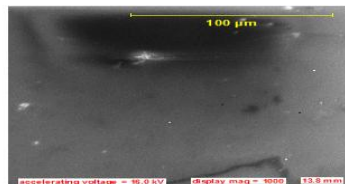
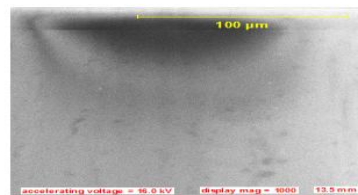


Figure 4.9a. SEM image of AgNPs at control (b) SEM image of AgNPs at 100°C

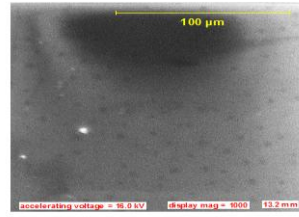
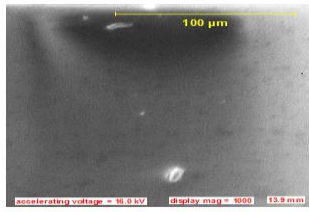


Figure 4.9 c. SEM image of AgNPs at 200⁰C (d) SEM image of AgNPs at 300⁰C

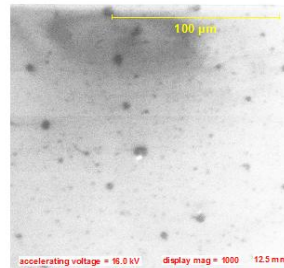
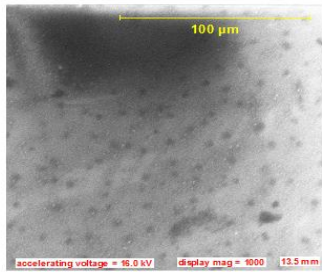


Figure 4.9 e. SEM image of AgNPs at 400⁰C (f) SEM image of AgNPs at 500⁰C

4.1.4 Optical and Electrical Characterization of Photoanode Device with Silver Nanoparticles/Titanium Dioxide

Table 4.1: Optical Characterization of each Photoanode Device

| Sample | Transmittance | Absorbance | Bandgap | Sheet Resistance |
|--------|---------------|------------|---------|------------------|
| A | 93.676 | 0.0289 | 2.65 | 85.746 |
| B | 92.700 | 0.0451 | 2.61 | 80.640 |
| C | 89.614 | 0.0768 | 2.60 | 72.465 |
| D | 87.402 | 0.0489 | 2.59 | 68.788 |
| E | 85.307 | 0.0568 | 2.48 | 63.893 |
| F | 88.105 | 0.0499 | 2.48 | 66.432 |

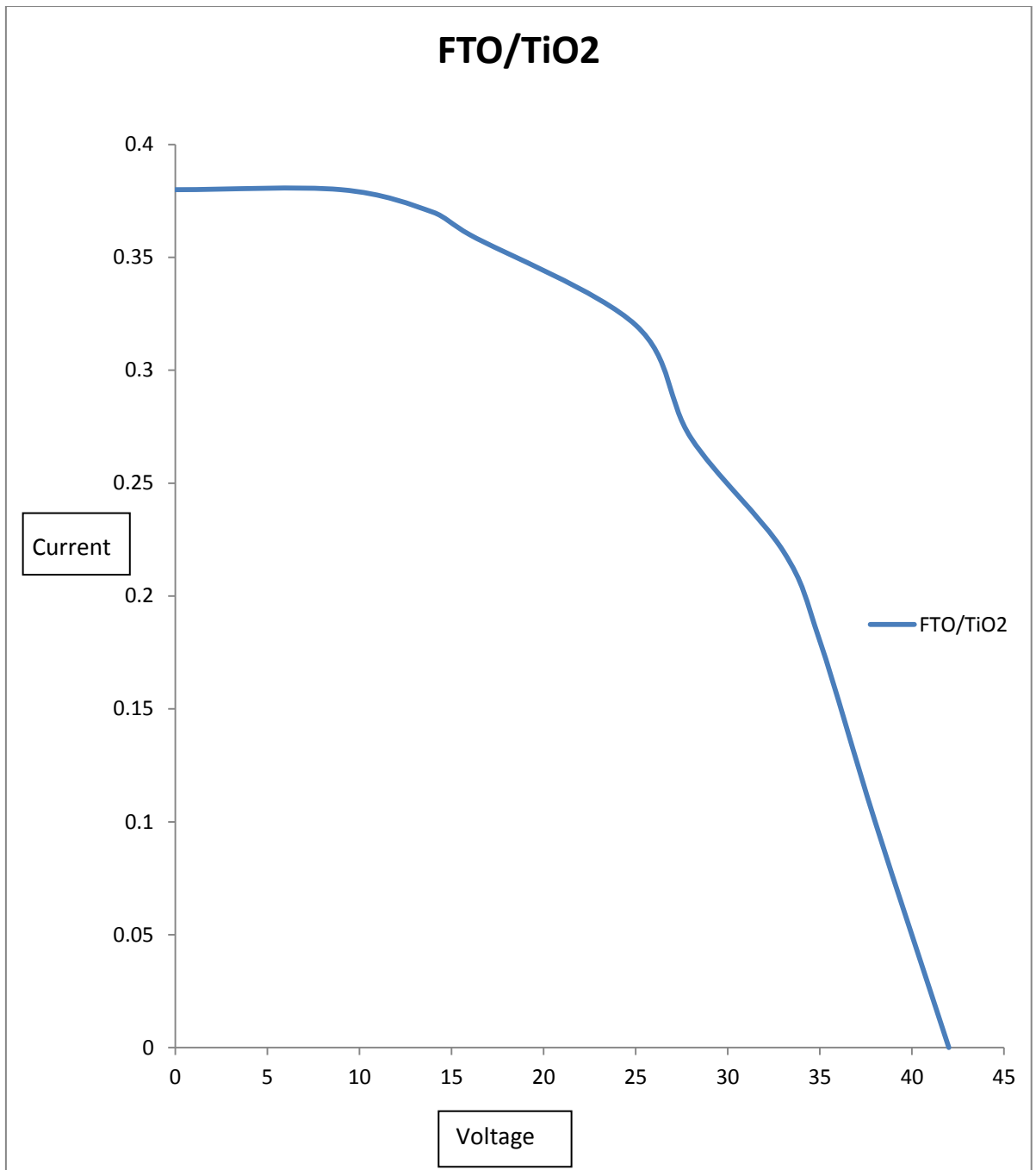


Fig. 4.10: Current -voltage characteristics of the DSSC without silver nanoparticles.

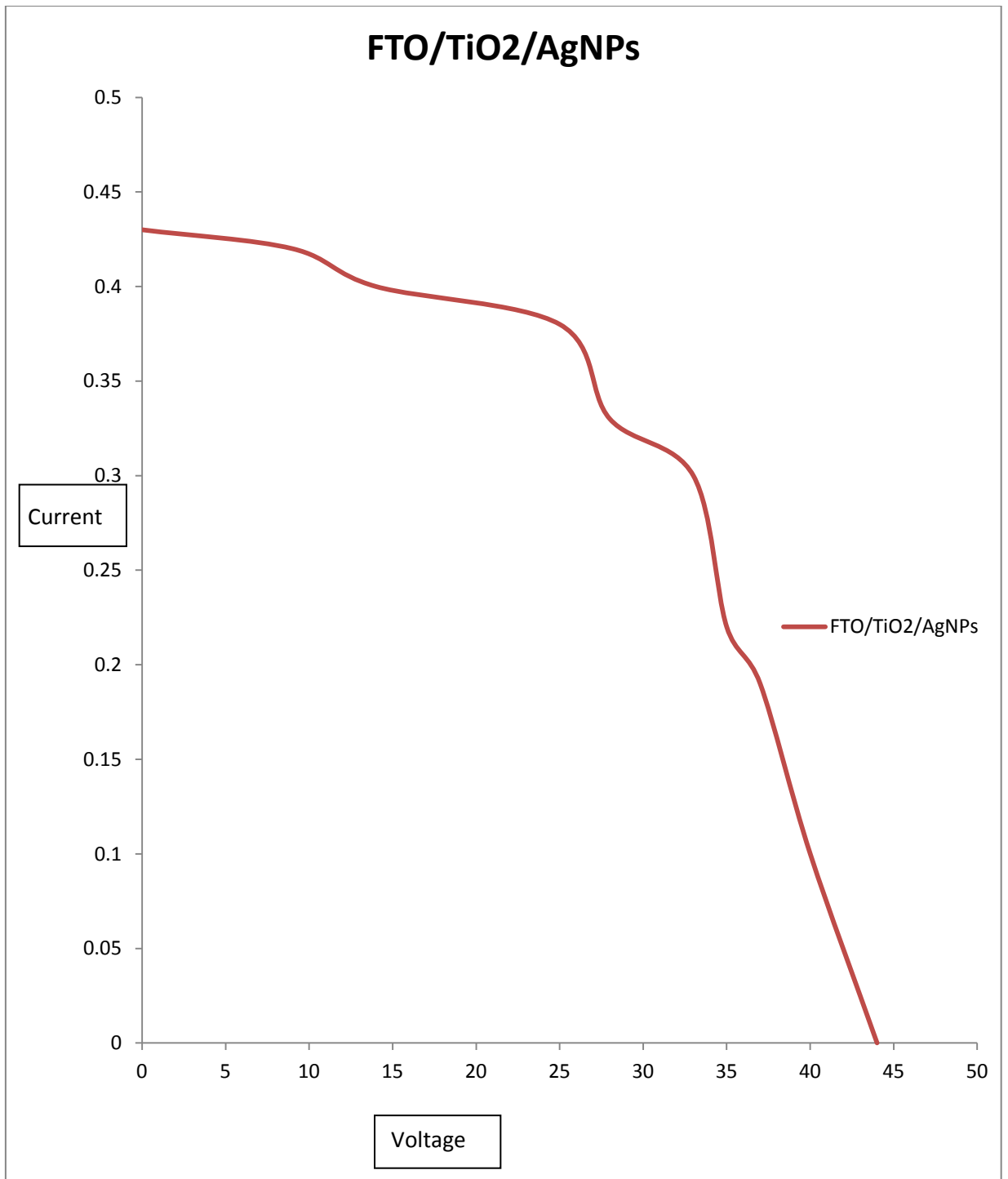


Fig. 4.11: Current -voltage characteristics of the DSSC with silver nanoparticles.

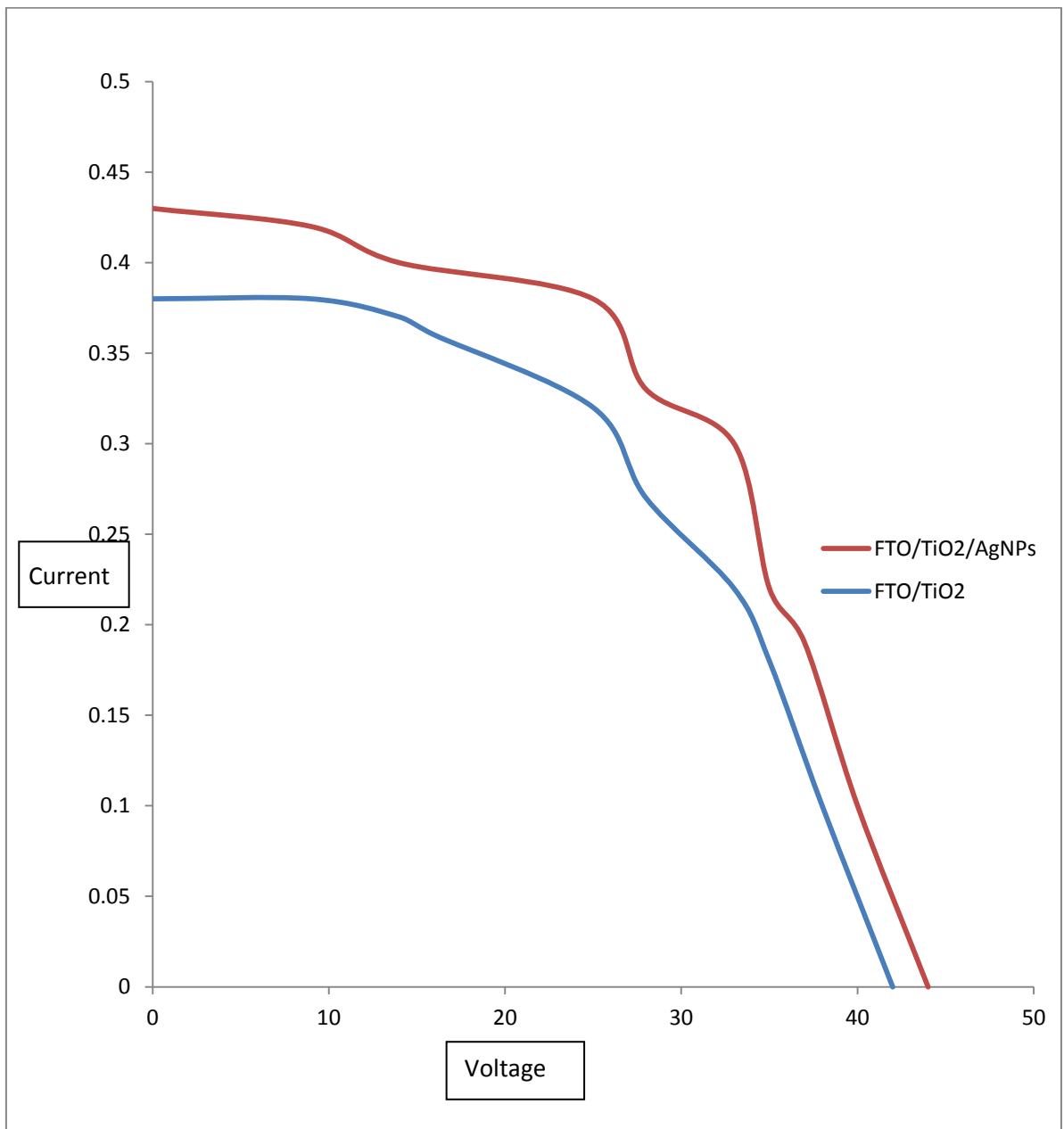


Fig. 4.12: Current-voltage characteristics of the DSSC with and without silver nanoparticles.

Table 4.2: Performance Characteristics of DSSCs Fabricated with Different Anodes

| DSSC | J _{sc} (mA/cm ²) | V _{oc} (V) | J _{max} (mA/cm ²) | V _{max} (V) | FF | η(%) |
|------------------------------|--|------------------------|---|----------------------|-------|-------|
| FTO/TiO ₂ | 0.38 | 42.00 | 0.36 | 25.00 | 0.564 | 8.90 |
| FTO/TiO ₂ / AgNPS | 0.43 | 44.00 | 0.40 | 25.80 | 0.546 | 10.32 |

4.2 Discussion

4.2.1 Optical Properties of Silver Nanoparticles

UV-visible spectroscopy is one of the most widely used techniques to study the optical characterization of Ag NPs. The absorption spectrum of the resonance peaks is taken on an FTO substrate to ensure that the interaction between the substrate and nanoparticles is minimized. Localized surface plasmons (SPs) are collective oscillations of the conduction electrons in metal particles. Movement of conduction electrons upon excitation with incident light leads to escalation of polarization charges on the particle surfaces.

This acts as a restoring force, allowing a resonance to occur at a particular frequency, which is termed the dipole surface plasmon resonance frequency. Incident light that is in the region of the resonance wavelength of the particles is strongly absorbed, depending on the size of the particles.

Reflectance Spectra

The reflectance spectra of silver nanoparticles films which are annealed at different temperature on glass substrates and control which was not annealed in the

wavelengths range of 100-1000nm are shown in Figure 4.1. After annealing, the reflectance decreased in silver nanoparticle films compared to the control.

Transmittance Spectra

The transmittance spectra of the silver nanoparticles films prepared at different annealing temperatures, in the wavelengths range of 100-1000nm are shown in Fig. 4.2. After annealing of the films the transmittance increases when compared to the control

Absorption Spectra

Fig.4.3 shows UV-VIS absorbance spectra of silver nanoparticles films, and the films annealed at different temperatures on glass substrates and that of the control (not annealed). The UV-VIS spectroscopy revealed the formation of silver nanoparticles by exhibiting the typical surface plasma on absorption maxima at 250nm for UV-VIS spectrum. A sharp peak was observed near 250 nm, after which there was a sharp decrease in absorption. Then there was a sharp increase in absorption and a bump appears on 350nm in the ultraviolet region and then it started decreases linearly up to visible region. In UV-VIS spectra, there was a decrease in absorption in visible region when compared to the control.

Figure 4.3 presents the surface plasmon absorption band in the range of 300-750 nm, with an absorption peak at 445 nm and with a broader peak at 645 nm. As there are various sizes of Ag NPs and the interparticle distances are pretty close to each other, this observation arises from coherent coupling between molecular excitons and electronic polarizations of noble-metal nanoparticles.

Bandgap Spectra of Silver nanoparticles Film

Figure 4.4 presents the bandgap spectra of Silver nanoparticles films, and the films annealed at different temperatures from 100°C to 500°C on glass substrates ranges from 3.90eV to 4.00eV and films not annealed showed a band gap of 3.86eV,

4.2.2 Optical Properties of Silver Nanoparticles/Titanium oxide Thin Film

Figure 4.5 the Reflectance spectra of mixed Silver nanoparticles and TiO₂ at different concentration films while Figure 4.6. the transmittance spectra of mixed Silver nanoparticles and TiO₂ at different concentration films. Fig. 4.7 shows the absorbance of the titanium dioxide and prepared Ag-NPs suspension with the dye within the wavelength range of 350-1000 nm. The relatively broad and strong enhancement is observed in the range of 370-650 nm with peaks at about 390 nm and 550 nm as shown in Fig. 4.7 (FTO/TiO₂/NPs-Ag) which coincides with the localized surface plasmon resonance (LSPR) band position of decorated Ag-NPs and a peak around 550 nm as shown in Fig. 4.4 (FTO/TiO₂). This enhanced absorption and broadened spectrum absorption range of the photoanode was mainly attributed to the LSPR of Ag-NPs, which interacted with the dye, enhancing dye absorption that resulted in more charge carrier generation. The absorption of the entire visible region for the anode with Ag-NPs was stronger than that for the anode without Ag-NPs, which was the product of two distinct effects. First, an absorption attributed to the surface plasmon resonance (SPR) of metallic silver nanoparticles in the TiO₂. Second, well-separated Ag-NPs with wide range of size and shape exhibits a broad and red shifted SP band, improving the absorption throughout the entire region. It is also seen from the figure 4.7 that UV-VIS absorbance spectra of TiO₂/AgNPs films is higher than the film without silver

nanoparticles (control), this was due to the surface plasmon resonance (SPR) of metallic silver nanoparticles in the TiO₂. It is also observed that the absorbance increases with increasing in silver nanoparticles concentration until optimum concentration was reached at 0.75ml.

Bandgap Spectra of TiO₂/Silver nanoparticles Film

Figure 4.8 displays the optical band gap of ratio of TiO₂/AgNPs films was smaller than those of pure TiO₂ due to effect of Silver nanoparticles. The band gap of mixed silver nanoparticles with titanium dioxide thin film at different concentration on glass substrate range from 3.70 to 3.80eV and films with TiO₂ only, it showed a band gap of 3.90eV.

Morphological Characterization

Figures 4.9 a-f show SEM images of silver nanoparticles deposited on glass substrate and annealed at different annealing temperatures and a film which was not annealed. The surface of silver nanoparticles without annealing was relatively smooth. A few holes have appeared after annealing from 100°C-500°C, the roughness of the surface of the sample increased as annealing temperature increased. The results showed that annealing temperature significantly influenced the size and shape of silver particles.

4.2.3 I-V Characteristics of DSSCs

The performance of the various DSSCs fabricated using the best sample of working electrodes obtained from specified factors considered are evaluated and presented in the Table 4.1 The graphical representation of the performance (I-V Characterizations) are also displayed in figure 4.10-4.12 . The parameters shorts circuit current (I_{sc}) and open circuit voltage (V_{oc}) of each cell were evaluated from it I-V curve.

The DSSCs output power was calculated using equation 3.2 .The maximum current I_m and voltage V_m Corresponding to the maximum power point were also obtained from I-V Curve .The Corresponding parameters fill factor(FF) and Efficiency (η) for each cell were evaluated using equation 3.3 and 3.4 respectively . The total result are presented in the Table 4.2 for both titanium dioxide with silver nanoparticles and the one without silver nanoparticles.

The total photon-to-current energy conversion efficiency, for the FTO/TiO₂ and FTO/TiO₂/Ag-NPs electrodes are 8.90% and 10.32%, respectively. , taking in to consideration the optimum thickness, dye-loading time, annealing temperature and annealing time as specification factors.

CHAPTER FIVE

CONCLUSION AND RECOMMENDATION

5.1 Conclusion

There are numerous ways of designing DSSC which may be done by changing photoanode material, cathode materials, natural and synthetic dye of different types and changing the electrolyte. Among these DSSC components, the photoanode plays a vital role in determining the DSSC performance. So far, a titanium dioxide (TiO_2) is one of the most commonly used photoanode materials, and it is promising material for a DSSC because of its low cost, ease of fabrication, relatively high energy conversion efficiency, high specific surface area, and non-toxicity. However, the major limitation associated with using TiO_2 as a photoanode is its random electron transport, which can cause the electron-hole recombination process and hence hinder the cell performance. In order to solve this serious issue, designing a photoanode with an efficient charge transport pathway from the photon injected carriers to the current collector seems to be a possible alternative to enhance the performance of DSSCs.

Silver nanoparticles have been introduced to the high-potential material for titanium dioxide based photoanode. The presence of silver nanoparticles synthesized using locally available materials, in the titanium dioxide film has given very significant effect towards its optical and electrical properties of anode for DSSCs. The size distribution and homogeneity of the silver nanoparticle film produce a good trend of surface plasmon resonance behavior of the particles. This behavior leads towards the improvement of the performance of the charge-carrying activity of the titanium dioxide photoanode system.

A TiO₂photoanode with an amount of Ag-NPswas investigated through preparation of TiO₂/Ag-NPs composite with different concentration of silver nanoparticles. The performance of the DSSC highly depends on the Silver nanoparticles. The result shows that adding Ag-NPs to TiO₂photoanode significantly improved the performance of the DSSC. The FTO/TiO₂/Ag-NP electrode presents an enhanced photocurrent response compared to the FTO/TiO₂ electrode.

The cell with FTO/TiO₂/Ag-NP electrode exhibited over 20% improvement over the photocurrent of FTO-based device lacking silver nanoparticles. The increase of I_{sc}forFTO/TiO₂/Ag-NPis attributed to the enhanced light absorption and broadened absorption spectral range of the composite photoanode due to the Surface Plasmon Resonance of the Ag-NPs, While the V_{oc} increase may be reasonably related to the more negative quasi-Fermi energy of the Ag-TiO₂ composite system due to the enhanced electron capture and storage capability resulting from Ag-NP doping.

5.2 Recommendation for Further Study

It is suggested that the enhanced photocurrent response was mainly attributed to plasmonic scattering which caused an apparent increase of the optical absorption of dye, resulting in a drastically enhanced photocurrent Thus, this result can be further used for photovoltaic application where more theoretical study will be carried out for better understanding of light trapping of these particles.

Experiments with metal nanoparticles embedded inside the semiconductor material, preferably near the junction depth, should be made in order to observe the near field effects on the direct charge carrier generation within solar cells.

REFERENCES

- Agglund, C.H., Ach, M.Z and Kasemo, B. (2008). Enhanced charge carrier generation in dye sensitized solar cells by nanoparticle Plasmon. *Applied Physics Letters*. 92:013113-1–013113-3.
- Ahn, N., Son, D.-Y., Jang, I.-H., Kang, S.M., Choi, M. and Park, N.-G. (2015). Highly Reproducible Perovskite Solar Cells with Average Efficiency of 18.3% and Best Efficiency of 19.7% Fabricated via Lewis Base Adduct of Lead(II) Iodide. *Journal of the American Chemical Society*, 137, 8696-8699.
- Alex, C., Mayer, Shawn, R., Scully, Brian, E., Hardin, Michael, W., Rowell and Michael, D. McGehee (2007) .Polymer-Based Solar Cells: A Review. *Materials Today*, 10, 28-33.
- Andorka, F. (2014). CIGS Solar Cells Simplified. Solar Power, World. <http://www.solarpowerworldonline.com/2014/01/cigs-solar-cells-simplified/>
- Asghar M. I., Miettunen K., Halme, J., Vahermaa P., Toivola M., Aitola K. and Lund P. (2010)“Review of stability for advanced dye solar cells,” *Energy and Environmental Science*, 3(4), 418-426.
- Atwater, H. A. and Polman, A., (2010) “Plasmonics for improved photovoltaic devices,” *Nature Materials*, 9(3), 205–213.
- Badawy, W.A. (2015). A Review on Solar Cells from Si-Single Crystals to Porous Materials and Quantum Dots. *Journal of Advanced Research*, 6, 123-132.
- Bagher, A.M., Vahid, M.M.A. and Mohsen, M. (2015).Types of Solar Cells and Application. *American Journal of Optics and Photonics*, 3, 94-113.
- Berginc, M., Opara Krasovec, U., Hocevar, M. and M. Topic, (2007).“Effect of masking and back reflector on performance of dye sensitized solar cells at different cell temperatures,” in *Proceedings of the 22nd European Photovoltaic Solar Energy Conference*, Milan, Italy.
- Bertolli, M. (2008).Solar Cell Materials. Course: Solid State II. Department of Physics, University of Tennessee, Knoxville.
- Capar, S. (2005) “Photovoltaic Power Generation for Polycrystalline Solar Cells and Turning Sunlight into Electricity Thesis,” Engineering Physics, University of Gaziantep.

- Castellano, R. (2010). Solar Panel Processing. Old City Publishing Inc., Philadelphia. Cell,” *Coordination Chemistry Reviews*, 248(13-14), 1381-1389.
- Catchpole, K. R. and Polman, A., (2008). “Plasmonic solar cells,” *Optics Express*, 16(26), 21793-21800.
- Chen X, Zhao C, Rothberg L. (2008). Plasmon enhancement of bulk hetero junction organic photovoltaic devices by electrode modification. *Applied Physics Letters* 93:123302.
- Chopra, K.L., Paulson, P.D. and Dutt, V. (2004). Thin-Film Solar Cells: An Overview. *Progress in Photovoltaic*, **12**, 69-92.
- Choubey, P.C., Oudhia, A. and Dewangan, R. (2012). A Review: Solar Cell Current Scenario and Future Trends. *Recent Research in Science and Technology*, 4, 99-101.
- Chu, Y. and Meisen, P. (2011). Review and Comparison of Different Solar Energy Technologies. Report of Global Energy Network Institute (GENI), Diego.
- Cole J.R and Halas N.J. (2006). Optimized plasmonic nanoparticles distributions for solar spectrum harvesting. *Applied Physics Letters* 89:153120.
- Eli, D., Onimisi, M. Y., Abdu, S. G., Gyuk, P. M. and Jonathan, E. (2016). Enhanced Performance of a Dye Sensitized Solar Cell Using Silver Nanoparticles Modified Photoanode, *Journal of Scientific Research & Reports* 10(4), 1-8.
- Dang, M.T, Want, Z.G., Bejbouji, H., Urien, M., Dautel, O.J., Vignau, L. and Hirsch, L. (2011). Polymeric solar cells based on P3HT: PCBM: Role of the casting solvent. *Solar Energy Materials and Solar Cells*. 95:3408-3418.
- Dubey, S., Sarvaiya, J.N. and Seshadri, B. (2013). Temperature Dependent Photovoltaic (PV) Efficiency and Its Effect on PV Production in the World: A Review. *Energy Procedia*, 33, 311-321.
- Elsabawy, K.M., El-Hawary, W.F. and Refat, M.S. (2012). Advanced Synthesis of Titanium-Doped-Tellurium-Cadmium Mixtures for High Performance Solar Cell Applications as One of Renewable Source of Energy. *International Journal of Chemical Sciences*, 10, 1869-1879.

- Fang, X., Ma, T., Guan, G., Akiyama, M., Kida, T. and Abe, E. "Effect of the thickness of the Pt film coated on a counter electrode on the performance of a dye-sensitized solar cell," *Journal*
- Furkan Dinçer and Mehmet Emin Meral (2010). Critical Factors that Affecting Efficiency of Solar Cells, *Smart Grid and Renewable Energy*, 2010, 1, 47-50
- Ganesh, B.N.V.S. and Supriya, Y.V. (2013). Recent Advancements and Techniques in Manufacture of Solar Cells: Organic Solar Cells. *International Journal of Electronics and Computer Science Engineering*, 2, 565-573.
- Goetzberger A., Hebling C. and Schock H.-W., (2003). "Photovoltaic Materials, History, Status and Outlook," *Materials Science and Engineering*, 40, 1-46.
- Graetzel, M., Janssen, R.A.J., Mitzi, D.B. and Sargent, E.H. (2012). Materials Interface Engineering for Solution-Processed Photovoltaics. *Nature*, 488, 304-312.
- Hagfeldt, A., Boschloo, G., Sun L., Kloo L. and Pettersson, H. (2010). "Dye-sensitized solar cells," *Chemical Reviews*, 110(11), 6595–6663.
- Hoppe, H. and Sariciftci, N.S. (2008). Polymer Solar Cells. *Advances in Polymer Science*, 214, 1.
- Hore, S., Vetter, C., Kern, R., Smit, H. and Hirsch, A. (2006) "Influence of scattering layers on efficiency of dye-sensitized solar cells," *Solar Energy Materials and Solar Cells*, 90(9), 1176–1188.
- Imamzai, M., Aghaei, M., Hanum, M.D., Thayoob, Y. and Forouzanfar, M. (2012). A Review on Comparison between Traditional Silicon Solar Cells and Thin-Film CdTe Solar Cells. *Proceedings of National Graduate Conference (Nat-Grad 2012)*, Tenaga Nasional University, Putrajaya Campus, 8-10 November 2012, 1-5.
- Ito, S., Zakeeruddin, S. M., Humphry-Baker R., Liska P., Charvet R., Comte P., Nazeeruddin M.K., Pechy P., Takata M., Miura H., Uchida S., Gratzel M. (2006). "High efficiency organic-dye-sensitized solar cells controlled by nanocrystalline-TiO₂ electrode thickness," *Advanced Materials*, 18, 1202-1205.
- Jayakumar, P. (2009) Solar Energy Resource Assessment Handbook. Renewable Energy Corporation Network for the Asia Pacific.

- Koo, H.J., Park, J., Yoo, B., Yoo, K., Kim, K. and Park, N. G. (2008). "Size dependent scattering efficiency in dye-sensitized solar cell," *Inorganica Chimica Acta*, vol. 361, no. 3, pp. 677-683.
- Kreibig U and Vollmer M. (1994). *Optical properties of metal clusters*. Springer, Berlin.; 77-88
- Kuang D., Klein C., Ito S., Wenger B., Moser J., Humphry-Baker R., Zakeeruddin S.M and Gratzel M. (2007). "High-Efficiency and stable mesoscopic dye-sensitized solar cells based on a high molar extinction coefficient ruthenium sensitizer and nonvolatile electrolyte," *Advanced Materials*, 19(8)1133-1137.
- Lagos, N, Sigala, M.M. and Lidorikis E. (2011). Theory of plasmonic near-field enhanced absorption in solar cells. *Applied Physics Letters*. 99:063304.
- Lee, J.K., Ma, W.L., Brabec, C.J., Yuen J, Moon, J.S., Kim, J.Y., Lee, K., Bazan, G.C. and Heeger A.J. (2008). Processing additives for improved efficiency from bulk hetero-junction solar cells. *Journal of the American Chemical Society*. 130: 3619–3623.
- Leroy, F. (2003). *A Century of Nobel Prize Recipients: Chemistry, Physics, and Medicine*. CRC Press, Hoboken. <http://dx.doi.org/10.1201/9780203014189>
- Li, G., Shrotriya V, Yao Y, Yang Y. (2005). Investigation of annealing effects and film thickness dependence of polymer solar cells based on poly(3-hexylthio-phenylene). *Journal of Applied Physics*. 98: 043704.
- Li, G., Zhu, R. and Yang, Y. (2012). Polymer Solar Cells. *Nature Photonics*, 6, 153-161.
- Li, P., Wu, J., Lin, J., Huang, M., Lan, Z. and Li, Q. (2008) "Improvement of performance of dye-sensitized solar cells based on electrodeposited-platinum counter electrode," *Electrochimica Acta*, 53 (12), 4161–4166.
- Lin, L. Y., Yeh, M. H., Lee C. P. Chang J. (2014) "Insights into the co-sensitizer adsorption kinetics for complementary organic dye sensitized solar cells," *Journal of Power Sources*, 247,.906

- Luque, A. and Hegedus, S. (2003). Handbook of Photovoltaic Science and Engineering, 2nd Edition, John Wiley & Sons, Ltd., Hoboken. <http://dx.doi.org/10.1002/0470014008>
- M. Gratzel, (2001). "Photoelectro chemical cells," *Nature*, 414(6861), 338–344,
- Ma, W., Yang, C., Gong, X., Lee, K. and Heeger, A.J. Thermally stable, efficient polymer solar
- Ma, X.J., Wu, J.Y., Sun Y.D. and Liu, S.-Q.(2009) "The Research on the Algorithm of Maximum Power Point Tracking in Photovoltaic Array of Solar Car," *Vehicle Power and Propulsion Conference, IEEE*, pp. 1379-1382.
- Maehlum, M.A. (2015) Energy Informative The Homeowner's Guide To Solar Panels, Best Thin Film Solar Panels-Amorphous, Cadmium Telluride or CIGS? Last updated 6 April 2015.
- Maruyama, T., Shinyashiki, Y. and Osako, S. (1998). "Energy Conversion Efficiency of Solar Cells Coated with Fluorescent Coloring Agent," *Solar Energy Materials & Solar Cells*, Elsevier Science.
- McEvoy, A., Castaner, L. and Markvart, T. (2012) Solar Cells: Materials, Manufacture and Operation. 2nd Edition, Elsevier Ltd., Oxford, 3-25.
- Mohanta, P. R., Patel, J., Bhuvra, J. and Gandhi, M. (2015) A Review on Solar Photovoltaics and Roof Top Application of It. *International Journal of Advanced Research in Science, Engineering and Technology*, 2, 2394-2444.
- Nabhani, N. and Emami, M. (2013) Nanotechnologies and Its Applications in Solar Cells. *International Conference on Mechanical and Industrial Engineering (ICMIE'2013)*, Penang, 28-29 August 2013, 88-91
- Nazeeruddin, M. K., Pechy, P. and Renouard T., Zakeeruddin S.M., Humphry-Bakar R., Comte P., Liska P., Cevey L., Costa E., Shklover V., Spiccia L., Deacon G.B., Bignozzi C.A. and Gratzel M. (2001) "Engineering of efficient panchromatic sensitizers for nanocrystalline TiO₂based solar cells," *Journal of the American Chemical Society*, 123(8), 1613–1624.
- Nishihata, M., Ishihara Y. and Todaka, T. (2006) "Presumption of Solar Power Generation Corresponding to the Change of Solar Spectrum, Photovoltaic Energy Conversion,"

- Noguez, C., (2007). "Surface Plasmon on metal nanoparticles: the influence of shape and physical environment," *Journal of Physical Chemistry C*, 111(10), 3606-3619.
- Nozik, A.J. (2010) Nanoscience and Nanostructures for Photovoltaics and Solar Fuels. *NANO Letters*, 10, 2735-2741. *Of Electro analytical Chemistry*, 570(2), 257-263, 2004.
- Pearsall N. M. and Hill, R. (2002) "Photovoltaic Modules, Systems and Applications," In: M. D. Archer, and R. Hill, Eds., *Clean Electricity from Photovoltaics*, World Science, 1, 1-42.
- Peplow, M. (2014) Organic Synthesis: The Robo-Chemist. *Nature*, 512, 20-22.
- Philipps, S.P., Bett, A.W., Horowitz, K. and Kurtz, S. (2015) Current Status of Concentrator Photovoltaics (CPV) Technology. Report Version 1.2, Fraunhofer Institute for Solar Energy Systems (NREL), September 2015. *Proceedings of the 2006 IEEE 4th World Conference*, Vol. 2, May 2006, pp. 2168-2171.
- Pillai, S. and Green, M. A. (2010) "Plasmonics for photovoltaic applications," *Solar Energy Materials and Solar Cells*, 94 (9), 1481-1486.
- Qin, C., Numata Y. and Zhang S. et al., (2013). "A near-infrared cis-configured squaraine co-sensitizer for high-efficiency dye sensitized solar cells," *Advanced Functional Materials*, 23, (30), 3782-3789.
- Queisser, H. J. and Werner, J. H., (1995). "Principles and Technology of Photovoltaic Energy Conversion," *Solid-State and Integrated Circuit Technology*, pp. 146-150.
- Rana, S. (2013). A Study on Automatic Dual Axis Solar Tracker System using 555 Timer. *International Journal of Scientific & Technology Research*, 1, 77-85.
- Razykov, T.M., Ferekides, C.S., Morel, D., Stefanakos, E., Ullal, H.S. and Upadhyaya, H.M. (2011). Solar Photovoltaic Electricity: Current Status and Future Prospects. *Solar Energy*, 85, 1580-1608.
- Saga, T. (2010) Advances in Crystalline Silicon Solar Cell Technology for Industrial Mass Production. *NPG Asia Materials*, 2, 96-102.

- Sethi, V.K., Pandey, M. and Shukla, P. (2011). Use of Nanotechnology in Solar PV Cell. *International Journal of Chemical Engineering and Applications*, 2, 77-80.
- Shi, D., Pootrakulchote, N., Li et al., (2008). "New efficiency records for stable dye-sensitized solar cells with low-volatility and ionic liquid electrolytes," *Journal of Physical Chemistry C*, 112(44), 17046–17050.
- Shi, D., Zeng, Y. and Shen, W. (2015) Perovskite/c-Si Tandem Solar Cell with Inverted Nanopyramids: Realizing High Efficiency by Controllable Light Trapping. *Scientific Reports*, 5, Article No. 16504.
- Srinivas, B., Balaji, S., NagendraBabu, M. and Reddy, Y.S. (2015). Review on Present and Advance Materials for Solar Cells. *International Journal of Engineering Research-Online*, 3, 178-182.
- Stenzel O, Stendal A, Voigtsberger K, Vonborczyskowski C. (1995). Enhancement of the photovoltaic conversion efficiency of copper phthalocyanine thin-film devices by incorporation of metal-clusters. *Solar Energy Materials and Solar Cells*.37: 337–348.
- Suhaimi, S., Shahimin, M.M., Alahmed, Z.A., Chyský, J. and Reshak, A.H. (2015). Materials for Enhanced Dye-Sensitized Solar Cell Performance: Electrochemical Application. *International Journal of Electrochemical Science*, 10, 28-59.
- Suita, Y. and Tadakuma, S. (2006). "Driving Performances of Solar Energy Powered Vehicle with MPTC," *IEEE*.
- Tachibana, Y., Hara, K., Sayama, K. and Arakawa, H. (2002). "Quantitative analysis of light-harvesting efficiency and electron-transfer yield in ruthenium-dye-sensitized nanocrystalline TiO₂ solar cells," *Chemistry of Materials*, vol. 14, no. 6, pp. 2527–2535.
- Temple, T. L., Mahanama, G. D. K., Reehal, H. S. and Bagnall, D.M., (2009) "Influence of localized surface plasmon excitation in silver nanoparticles on the performance of silicon solar cells," *Solar Energy Materials and Solar Cells*, 93(11), 1978–1985.
- Tina Casey (2015). An Article on Perovskites Will Power New Low-Cost & Highly Efficient Solar Cells. Clean Technical, 3 July 2015.

- Wai, R. J., Wang, W. H. and Lin, C.Y. “High-Performance Stand-Alone Photovoltaic Generation System,” *Proceedings of IEEE Transactions on Industrial Electronics*, Vol.
- Wall, A. (2014). Advantages and Disadvantages of Solar Energy. Process Industry Forum, 7 August 2013. Web. 2 February 2014.
- Wang, P., Zakeeruddin, S. M., Moser, J. E., Nazeeruddin, M. K., Sekiguchi, T. and Gratzel, M. (2003) “A stable quasi-solid-state dye sensitized solar cell with an amphiphilic ruthenium sensitizer and polymer gel electrolyte,” *Nature Materials*, 2(6), 402-407.
- Westphalen M, Kreibig U, Rostalski J, Luth H and Meissner D. (2000). Metal cluster enhanced organic solar cells. *Solar Energy Materials and Solar Cells*. 61:97–105.
- Whitburn, G. (2012). Exploring Green Technology, Fundamental Advantages and Disadvantages of Solar Energy.
- Wu, Y. and Gorder, P.F. (2014). Nature Communications. Published on 3 October, 2014.
- Wudl, F. and Srdanov, G. (1993). Conducting Polymer Formed of Poly (2-Methoxy-5-(2'-Ethylhexyloxy)-P-Phenylene Vinylene). US Patent 5,189,136.
- Yadav, A. and Kumar, P. (2015) Enhancement in Efficiency of PV Cell through P&O Algorithm. *International Journal for Technological Research in Engineering*, 2, 2642-2644.
- Yella A., Lee H.W. and Tsao H. N. et al., (2011). “Porphyrin-sensitized solar cells with cobalt (II/III)-based redox electrolyte exceed 12 percent efficiency,” *Science*, 334(6056), 629–634.
- Yogi Goswami, D. and Kreith, F. (2007). Handbook of Energy Efficiency and Renewable Energy. CRC Press, Boca Raton.
- Zhang, D., Wang, M., Alexandre, G., Brolo, JieShen, Li, X. and Huang, S. (2014). Enhanced performance of dyesensitized solar cells using gold nanoparticles modified fluorine tin oxide electrodes. *J. Phys. D: Applied Physics*. 2013; 46:024005:8.4812-4819, 2013.491-499.

- Zhang, S., Islam, A. and Yang X.et al., “Improvement of spectral response by co-sensitizers for high efficiency dye-sensitized solar cells,” *Journal of Materials Chemistry A*, 1(15).
- Zhang, S., Yang, X., Qin, C., Numata, Y. and Han, L. (2014). “Interfacial engineering for dye sensitized solar cells,” *Journal of Materials Chemistry A*.
- Zhu, J., Xue, M., Shen, H., Wu, Z., Kim, S., Ho, J.J., Hassani-Afshar, A., Zeng, B. and Wang K.L., (2011). Plasmonic effects for light concentration inorganic photovoltaic thin films induced by hexagonal periodic metallic nanospheres. *Applied Physics Letters* .98:151110- 1–151110-3.
- Zhu, R., Kumar, A. and Yang, Y. (2011). Polarizing Organic Photovoltaics. *Advanced Materials*, 23, 4193-4198.